

Data Fusion for Multipath-Based SLAM: Combining Information from Multiple Propagation Paths

Erik Leitinger *Member, IEEE*, Alexander Venus *Student Member, IEEE*,
Bryan Teague *Member, IEEE*, Florian Meyer *Member, IEEE*

Abstract—Multipath-based simultaneous localization and mapping (SLAM) is an emerging paradigm for accurate indoor localization with limited resources. The goal of multipath-based SLAM is to detect and localize radio reflective surfaces to support the estimation of time-varying positions of mobile agents. Radio reflective surfaces are typically represented by so-called virtual anchors (VAs), which are mirror images of base stations at the actual surfaces. In existing multipath-based SLAM methods, a VA is introduced for each propagation path, even if the goal is to map the reflective surfaces. The fact that not every reflective surface but every propagation path is modeled by a VA, complicates a consistent combination “fusion” of statistical information across multiple paths and base stations and thus limits the accuracy and mapping speed of existing multipath-based SLAM methods. In this paper, we introduce an improved statistical model and estimation method that enables data fusion for multipath-based SLAM by representing each surface by a single master virtual anchor (MVA). We further develop a particle-based sum-product algorithm (SPA) that performs probabilistic data association to compute marginal posterior distributions of MVA and agent positions efficiently. A key aspect of the proposed estimation method based on MVAs is to check the availability of single-bounce and double-bounce propagation paths at a specific agent position by means of ray-launching. The availability check is directly integrated into the statistical model by providing detection probabilities for probabilistic data association. Numerical results based on simulated and real data demonstrate significant improvements in estimation accuracy compared to state-of-the-art multipath-based SLAM methods.

I. INTRODUCTION

Emerging sensing technologies and innovative signal processing methods exploiting multipath propagation will lead to new capabilities for autonomous navigation, asset tracking, and situational awareness in future communication networks. Multipath-based simultaneous localization and mapping (SLAM) is a promising approach for obtaining position information of transmitters and receivers as well as information on their propagation environments. In multipath-based SLAM, specular reflections of radio signals at flat surfaces are modeled by virtual anchors (VAs) that are mirror images of base stations, called physical anchors (PAs) [1]. Typically, the number of VAs and their positions are unknown. Multipath-based SLAM methods can detect and localize VAs and jointly estimate the time-varying position of mobile agents [1]–[5]. The availability of VA location information makes it possible

to leverage multiple propagation paths of radio signals for agent localization and can thus significantly improve localization accuracy and robustness [6]–[9].

A. State of the Art

Multipath-based SLAM follows a feature-based SLAM approach [10]–[15], i.e., a map is represented by static VAs which are features to be mapped [3]–[5], [16], [17]. Most existing methods for multipath-based SLAM make use of parameter estimates related to multipath components, such as distances (which are proportional to delays), angles-of-arrival (AoAs), or angles-of-departure (AoDs) [18]–[20] as input. These parameters, considered as “measurements” by multipath-based SLAM, are estimated from received RF signals in a preprocessing stage [21]–[24].

A complicating factor in feature-based SLAM is measurement origin uncertainty, i.e., the unknown association of measurements with features [3]–[5], [20], [25]. In particular, (i) it is not known which map feature was generated by which measurement, (ii) there are missed detections due to low signal-to-noise-ratio (SNR) or occlusion of features, and (iii) there are false positive measurements due to clutter. Thus, an important aspect of multipath-based SLAM is *data association* (DA) between these measurements and the VA. Probabilistic data association can increase the robustness and accuracy of multipath-based SLAM but introduces additional unknown parameters. State-of-the-art methods for multipath-based SLAM are Bayesian estimators that perform the sum-product algorithm (SPA) on a factor graph [3]–[5] to avoid the curse of dimensionality related to the high-dimensional parameters space. Since the measurement models of multipath-based SLAM are nonlinear, most methods typically rely on sampling techniques [1]–[6]. Recently, multipath-based SLAM based on data collected by radios with ultra-wide bandwidth [26] or multiple antennas [2], [4], [27] was applied to indoor scenarios.

In existing methods for multipath-based SLAM, each VA represents a single propagation path from an agent to a PA. In particular, even if a reflective surface takes part in multiple propagation paths, each path is represented by a VA, and each VA is estimated independently [1]–[6], [28], [29]. The fact that not every reflective surface but every propagation path is modeled by a VA complicates a consistent combination “fusion” of statistical information across multiple propagation paths and PAs. It thus limits the accuracy and mapping speed of existing multipath-based SLAM.

B. Contributions and Notations

In this paper, we introduce a new statistical model that considers single-bounce and double-bounce propagation paths and

E. Leitinger and A. Venus are with the Signal Processing and Speech Communication Laboratory, Graz University of Technology, Graz, Austria, and the Christian Doppler Laboratory for Location-aware Electronic Systems (e-mail: (erik.leitinger,a.venus)@tugraz.at). B. Teague is with the MIT Lincoln Laboratory, Lexington, MA, USA (bryan.teague@ll.mit.edu). F. Meyer is with the Department of Electrical and Computer Engineering and Scripps Institution of Oceanography, University of California San Diego, San Diego, CA, USA (e-mail: fmeyer@ucsd.edu). This material is based upon work supported by the Under Secretary of Defense for Research and Engineering under Air Force Contract No. FA8702-15-D-0001 and the TU Graz.

enables data fusion for multipath-based SLAM. Contrary to existing multipath-based SLAM models, which represent propagation paths as SLAM features called VAs, in the proposed model, every reflective surface is represented by a SLAM feature referred to as master virtual anchor (MVA). Following the new MVA-based model, a factor graph is established, and an extension of the SPA multipath-based SLAM methods in [3]–[5] is developed. The resulting SPA makes it possible to infer reflective surfaces by combining information provided by multiple propagation paths and PAs. We also present a particle-based implementation of the proposed SPA that performs ray-launching to determine the availability of each single-bounce and double-bounce propagation at a specific agent position. The availability check is directly integrated into the statistical model, i.e., it determines detection probabilities used for probabilistic data association. The resulting multipath-based SLAM method can provide fast and accurate estimates of a large number of reflective surfaces and mobile agent positions. The key contributions of this paper are as follows.

- We introduce a statistical model and factor graph for multipath-based SLAM that considers single- and double-bounce propagation paths and facilitates data fusion.
- We extend the SPA for multipath-based SLAM [3]–[5] to the introduced factor graph to establish data fusion for multipath-based SLAM.
- We present a particle-based implementation that directly performs ray-launching to determine the availability of each single-bounce and double-bounce propagation path.
- We demonstrate significant improvements in estimation performance compared to existing multipath-based SLAM methods based on simulated and real data.

This paper advances over the preliminary account of our method provided in the conference publications [30], [31] by (i) extending the MVAs model to double-bounce propagation paths, (ii) introducing ray-launching to determine the availability of paths, (iii) presenting a detailed derivation of the factor graph, (iii) discussing a particle-based implementation, and (iv) demonstrating performance advantages compared to the classical multipath-based SLAM [3], [4].

Notation: Random variables are displayed in sans serif, upright fonts; their realizations in serif, italic fonts. Vectors and matrices are denoted by bold lowercase and uppercase letters, respectively. For example, a random variable and its realization are denoted by \mathbf{x} and x , respectively, and a random vector and its realization by \mathbf{x} and \mathbf{x} , respectively. Furthermore, $\|\mathbf{x}\|$ and \mathbf{x}^T denote the Euclidean norm and the transpose of vector \mathbf{x} , respectively, and $\langle \mathbf{x}, \mathbf{y} \rangle$ denotes the inner-product between the vectors \mathbf{x} and \mathbf{y} ; \propto indicates equality up to a normalization factor; $f(\mathbf{x})$ denotes the probability density function (PDF) of random vector \mathbf{x} (this is a short notation for $f_{\mathbf{x}}(\mathbf{x})$); $f(\mathbf{x}|\mathbf{y})$ denotes the conditional PDF of random vector \mathbf{x} conditioned on random vector \mathbf{y} (this is a short notation for $f_{\mathbf{x}|\mathbf{y}}(\mathbf{x}|\mathbf{y})$). The four-quadrant inverse tangent of position $\mathbf{p} = [p_1 \ p_2]^T$ is denoted as $\text{atan2}(p_2, p_1)$. The cardinality of a set \mathcal{X} is denoted as $|\mathcal{X}|$. Finally, $\delta(e)$ denotes the indicator function of the event $e = \mathbf{0}$ (i.e., $\delta(e) = 1$ if $e = \mathbf{0}$ and $\mathbf{0}$ otherwise).

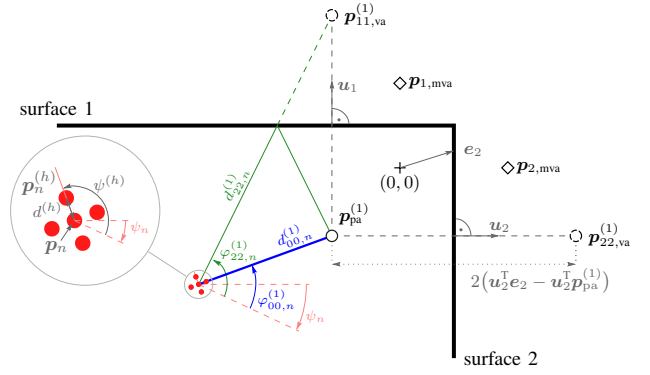


Fig. 1. A graphical depiction of a scenario involving $S = 2$ reflective surface, $J = 1$ PAs, and positions of the agent \mathbf{p}_n at time step n .

II. GEOMETRICAL RELATIONS

We consider a mobile agent equipped with an H -element antenna array and J PAs with known positions $\mathbf{p}_{\text{pa}}^{(j)} = [p_{1,\text{pa}}^{(j)} \ p_{2,\text{pa}}^{(j)}]^T \in \mathbb{R}^2$, $j \in \{1, \dots, J\}$, where J is assumed to be known, in an environment described by S reflective surfaces with index $s \in \mathcal{S} \triangleq \{1, \dots, S\}$. At every discrete time step n , the element locations are denoted by $\mathbf{p}_n^{(h)}$, $h \in \{1, \dots, H\}$, the agent position \mathbf{p}_n refers to the center of gravity of the array. We also define $d^{(h)} = \|\mathbf{p}_n^{(h)} - \mathbf{p}_n\|$ and $\psi^{(h)} = \text{atan2}(p_{2,n}^{(h)} - p_{2,n}, p_{1,n}^{(h)} - p_{1,n}) - \psi_n$, the distance from the reference location \mathbf{p}_n and the orientation, respectively, of the h -th element as shown in Fig. 1. At each discrete time slot n , the position $\mathbf{p}_n \in \mathbb{R}^2$ and the array orientation ψ_n of the mobile agent are unknown. The mobile agent transmits a radio signal, and the PAs act as receivers.¹ The radio signal arrives at the receiver via a line-of-sight (LOS) path as well as via multipath components (MPCs) originating from the reflection of surrounding objects.

We restrict the representation to MPCs related to single-bounce and double-bounce propagation paths. In particular, associated with PA j there are $|\mathcal{D}_S| = S$ single-bounce VAs [3], [32] at unknown positions $\mathbf{p}_{ss,\text{va}}^{(j)} \in \mathbb{R}^2$ with index $(s, s) \in \mathcal{D}_S \triangleq \{(s, s) \in \mathcal{S} \times \mathcal{S}\}$ and $|\mathcal{D}_D| = S(S-1)$ double-bounce VAs at unknown positions $\mathbf{p}_{ss',\text{va}}^{(j)} \in \mathbb{R}^2$ with index $(s, s') \in \mathcal{D}_D \triangleq \{(s, s') \in \mathcal{S} \times \mathcal{S} | s \neq s'\}$. Therefore, the maximum number of VAs for PA j is given by $|\mathcal{D}| = S + S(S-1)$ with $\mathcal{D} \triangleq \{(s, s') \in \mathcal{S} \times \mathcal{S}\} = \mathcal{D}_D \cup \mathcal{D}_S$.² By applying the image-source model [32], [33], a VA associated with a single-bounce propagation path is the mirror image of $\mathbf{p}_{\text{pa}}^{(j)}$ at reflective surface $s \in \mathcal{S}$ given by

$$\mathbf{p}_{ss,\text{va}}^{(j)} = \mathbf{p}_{\text{pa}}^{(j)} + 2(\mathbf{u}_s^T \mathbf{e}_s - \mathbf{u}_s^T \mathbf{p}_{\text{pa}}^{(j)}) \mathbf{u}_s \quad (1)$$

where $(s, s) \in \mathcal{D}_S$, \mathbf{u}_s is the normal vector of reflective surface s , and \mathbf{e}_s is an arbitrary point on this surface. The second summand in (1) represents the normal vector w.r.t. to reflective surface s in direction \mathbf{u}_s with the length of two times the distance between PA j at position $\mathbf{p}_{\text{pa}}^{(j)}$ and the normal-point at the reflective surface s , i.e., $2(\mathbf{u}_s^T \mathbf{e}_s - \mathbf{u}_s^T \mathbf{p}_{\text{pa}}^{(j)})$. By again applying the image-source model [32], [33] for VA at position

¹However, the proposed algorithm can be easily reformulated for the case where the PAs act as transmitters and the mobile agent acts as a receiver.

²Note that subscript indices denoted as $(\cdot)_{ss'}$ indicate variables related to potential MVAs (PMVAs) pairs (s, s') .

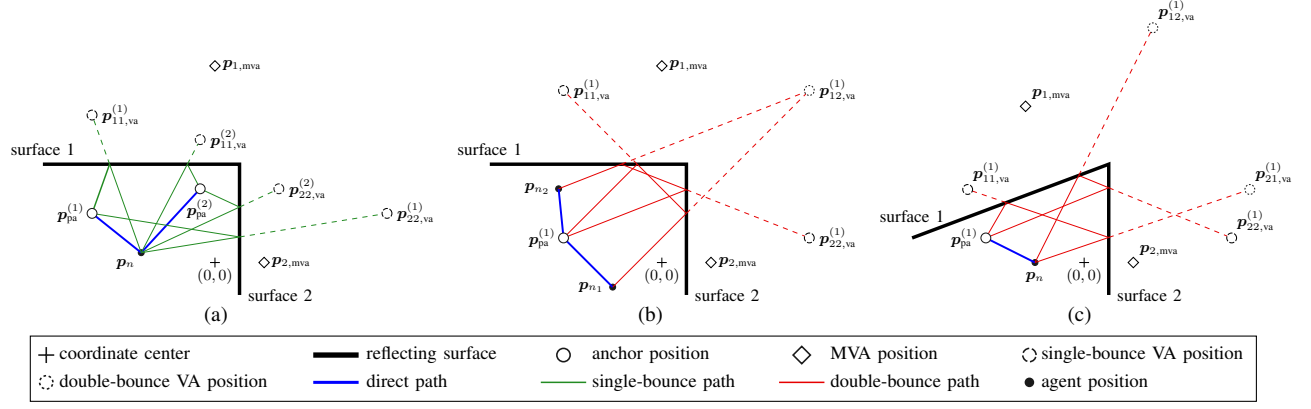


Fig. 2. A graphical depiction of a scenario involving $S = 2$ reflective surface (a) with perpendicular reflective surfaces, two PAs at positions $\mathbf{p}_{\text{pa}}^{(1)}$ and $\mathbf{p}_{\text{pa}}^{(2)}$, and the agent at position \mathbf{p}_n at time n , (b) with perpendicular reflective surfaces, one PA at positions $\mathbf{p}_{\text{pa}}^{(1)}$ and the agent at positions \mathbf{p}_n at time $n \in \{n_1, n_2\}$, and (c) with acute angle between the reflective surfaces, one PAs at positions $\mathbf{p}_{\text{pa}}^{(1)}$ and the agent at position \mathbf{p}_n at time n .

$\mathbf{p}_{s's',\text{va}}^{(j)}$ another VA that is obtained as the mirror image of $\mathbf{p}_{ss',\text{va}}^{(j)}$ at surface s , i.e.,

$$\mathbf{p}_{ss',\text{va}}^{(j)} = \mathbf{p}_{s's',\text{va}}^{(j)} + 2(\mathbf{u}_s^T \mathbf{e}_s - \mathbf{u}_s^T \mathbf{p}_{s's',\text{va}}^{(j)}) \mathbf{u}_s \quad (2)$$

where $(s, s') \in \mathcal{D}_D$. This VA represents a double-bounce propagation path. For conveniently addressing PA-related variables and factors, we also define $\mathbf{p}_{00,\text{va}}^{(j)} \triangleq \mathbf{p}_{\text{pa}}^{(j)}$ and $\tilde{\mathcal{D}} = (0, 0) \cup \mathcal{D}$. The distances and angle-of-arrivals (AOAs) related to the propagation paths at the agent position \mathbf{p}_n represented by $\mathbf{p}_{ss',\text{va}}^{(j)}$ with $(s, s') \in \tilde{\mathcal{D}}$ are modeled by $d_{ss',n}^{(j)} = \|\mathbf{p}_n - \mathbf{p}_{ss',\text{va}}^{(j)}\|$ and $\varphi_{ss',n}^{(j)} = \text{atan2}(p_{2,n} - p_{1,ss',\text{va}}^{(j)}, p_{1,n} - p_{1,ss',\text{va}}^{(j)}) - \psi_n$. Note that the distance $d_{00,n}^{(j)}$ and the AOAs $\varphi_{00,n}^{(j)}$ are the parameters related to the LOS path agent at position \mathbf{p}_n – PA j at position $\mathbf{p}_{\text{pa}}^{(j)}$. An example is shown in Fig. 1.

Note that the LOS path is associated with the PA itself. Due to blockage of propagation paths or geometrical restrictions between the reflective surfaces lead to availability constraints of propagation paths to certain VA positions [32]. Especially, double-bounce paths and their corresponding VA positions have limited availability depending on the mobile agent position \mathbf{p}_n (see Fig. 2b and Fig. 2c). Therefore, the number of available VAs for PA j is smaller than $|\mathcal{D}| = S + S(S-1)$. The proposed algorithm performs an availability check of each path using *ray-launching* [32] to determine whether a VA provides information as it is detailed in Section III-D.

A. MVA-Based Model of the Environment

A reflective surface is involved in multiple propagation paths, thus giving rise to multiple VAs. To enable the consistent combination, i.e., “fusion” of map information provided by distance measurement of different PAs, we represent reflective surfaces by S unique MVAs at unknown positions $\mathbf{p}_{s,\text{mva}} \in \mathbb{R}^2$, $s \in \mathcal{S}$. The unique MVA position $\mathbf{p}_{s,\text{mva}} \in \mathbb{R}^2$ is defined as the mirror image of $[0, 0]^T$ on the reflective surface S . By using some algebra, the transformation from MVA at $\mathbf{p}_{s,\text{mva}}$ to a VA at $\mathbf{p}_{ss,\text{va}}^{(j)}$ can be obtained as

$$\begin{aligned} \mathbf{p}_{ss,\text{va}}^{(j)} &= h_{\text{va}}(\mathbf{p}_{s,\text{mva}}, \mathbf{p}_{\text{pa}}^{(j)}) \\ &= -\left(\frac{2\langle \mathbf{p}_{s,\text{mva}}, \mathbf{p}_{\text{pa}}^{(j)} \rangle}{\|\mathbf{p}_{s,\text{mva}}\|^2} - 1\right) \mathbf{p}_{s,\text{mva}} + \mathbf{p}_{\text{pa}}^{(j)}. \end{aligned} \quad (3)$$

The transformation from MVAs at $\mathbf{p}_{s,\text{mva}}$ and $\mathbf{p}_{s',\text{mva}}$ to a double-bounce VA at $\mathbf{p}_{ss',\text{va}}^{(j)}$ can be obtained by applying (3) twice, i.e., $\mathbf{p}_{ss',\text{va}}^{(j)} = h_{\text{va}}(\mathbf{p}_{s,\text{mva}}, h_{\text{va}}(\mathbf{p}_{s',\text{mva}}, \mathbf{p}_{\text{pa}}^{(j)}))$. Similarly, the inverse transformation from a VA to a MVA position is given by

$$\begin{aligned} \mathbf{p}_{s,\text{mva}} &= h_{\text{mva}}(\mathbf{p}_{ss,\text{va}}, \mathbf{p}_{\text{pa}}^{(j)}) \\ &= \frac{\|\mathbf{p}_{\text{pa}}^{(j)}\|^2 - \|\mathbf{p}_{ss,\text{va}}^{(j)}\|^2}{\|\mathbf{p}_{\text{pa}}^{(j)} - \mathbf{p}_{ss,\text{va}}^{(j)}\|^2} (\mathbf{p}_{\text{pa}}^{(j)} - \mathbf{p}_{ss,\text{va}}^{(j)}). \end{aligned} \quad (4)$$

Note that the inverse transformation in (4) is used to determine a proposal distribution for the MVA states as described in Section V. Details of the derivation are provided in the supplementary material [34, Sec. I-A]. As an example, Fig. 2 shows three scenarios with two reflective surfaces described by two MVAs at positions $\mathbf{p}_{1,\text{mva}}$ and $\mathbf{p}_{2,\text{mva}}$. Fig. 2a shows a scenario with two PAs $j \in \{1, 2\}$, the according VAs, and an agent at position \mathbf{p}_n . Each PA generates one VA associated with a single-bounce propagation path. Fig. 2b shows a scenario with one PA, the corresponding VAs associated with single-bounce and double-bounce propagation paths, and an agent at two positions \mathbf{p}_{n1} and \mathbf{p}_{n2} . Note that in scenarios with perpendicular surfaces, the order of the surfaces, i.e., surface s – surface s' or surface s' – surface s does not influence the calculation of the VA-position associated with the double-bounce propagation path. Depending on the agent position \mathbf{p}_n , only one double-bounce propagation path (related to one of the two orders) is available (Section III-D). Fig. 2b shows a scenario with non-perpendicular surfaces. In this case, different “bounce orders” lead to different VA-positions. In particular, if there is an acute angle between a pair of reflecting surfaces, there exist regions of agent locations \mathbf{p}_n for which two double-bounce propagation paths are available at the same time (cf. Section III-D). These regions depend on the PA position as well as the angle between the two surfaces.

III. SYSTEM MODEL

At each time n , the state of the agent $\mathbf{x}_n = [\mathbf{p}_n^T \mathbf{v}_n^T \psi_n]^T$, where \mathbf{v}_n is the agent velocity. We assume that the array is rigidly coupled with the movement direction. As in [3],

[35], [36], we account for the unknown number of MVAs by introducing PMVAs $s \in \mathcal{S}_n \triangleq \{1, \dots, S_n\}$. The number S_n of PMVAs is the maximum possible number of actual MVA that produced a measurement so far [3], [36] (where S_n increases with time). PMVA states are denoted as $\mathbf{y}_{s,n} = [\mathbf{p}_{s,\text{mva}}^T r_{s,n}]^T$. The existence/nonexistence of PMVA s is modeled by the existence variable $r_{s,n} \in \{0, 1\}$ in the sense that PMVA s exists if and only if $r_{s,n} = 1$. It is considered also if PMVA s is nonexistent, i.e., if $r_{s,n} = 0$. The states $\mathbf{p}_{s,\text{mva}}^T$ of nonexistent PMVAs are obviously irrelevant. Therefore, all PDFs defined for PMVA states, $f(\mathbf{y}_{s,n}) = f(\mathbf{p}_{s,\text{mva}}, r_{s,n})$, are of the form $f(\mathbf{p}_{s,\text{mva}}, 0) = f_{s,n} f_d(\mathbf{p}_{s,\text{mva}})$, where $f_d(\mathbf{p}_{s,\text{mva}})$ is an arbitrary “dummy PDF” and $f_{s,n} \in [0, 1]$ is a constant and can be interpreted as the probability of non-existence [3], [36].

We also define the number of VAs for each PA given as $|\mathcal{D}_n^{(j)}| = S_n^{(j)} + S_n^{(j)}(S_n^{(j)} - 1)$ with $\mathcal{D}_n^{(j)} \in \{(s, s') \in \mathcal{S}_n \times \mathcal{S}_n\} = \mathcal{D}_{S,n}^{(j)} \cup \mathcal{D}_{D,n}^{(j)}$ and $\tilde{\mathcal{D}}_n^{(j)} = (0, 0) \cup \mathcal{D}_n^{(j)}$.

A. Measurements and New PMVAs

The distance and AOA measurements³ related to the path agent at position \mathbf{p}_n – VA at position $\mathbf{p}_{ss',\text{va}}^{(j)}$ with $(s, s') \in \tilde{\mathcal{D}}_n$ are given by

$$z_{d,m,n}^{(j)} = \|\mathbf{p}_n - \mathbf{p}_{ss',\text{va}}^{(j)}\| + v_{\tau m,n}^{(j)} \quad (5)$$

$$z_{\varphi m,n}^{(j)} = \text{atan2}(p_{2,n} - p_{2,ss',\text{va}}^{(j)}, p_{1,n} - p_{1,ss',\text{va}}^{(j)}) - \phi_n + v_{\varphi m,n}^{(j)} \quad (6)$$

where $v_{\tau m,n}^{(j)}$ and $v_{\varphi m,n}^{(j)}$ are, respectively, zero-mean Gaussian measurement noises with standard deviations $\sigma_{\tau m,n}^{(j)}$ and $\sigma_{\varphi m,n}^{(j)}$. The measurements are combined in the vector $\mathbf{z}_{m,n}^{(j)} = [z_{d,m,n}^{(j)} z_{\varphi m,n}^{(j)}]^T$ with $m \in \mathcal{M}_n^{(j)} \triangleq \{1, \dots, M_n^{(j)}\}$ for PA j . Note that before measurements are acquired, the number of measurements $M_n^{(j)}$ is a priori random.

LOS path likelihood function: Using (5), (6), and $\mathbf{p}_{00,\text{va}}^{(j)} = \mathbf{p}_{\text{pa}}^{(j)}$, we can directly obtain the likelihood function for the LOS path as $f(\mathbf{z}_{m,n}^{(j)} | \mathbf{p}_n)$.

Single-bounce path likelihood function: Using (5), (6), and the transformation in (3), i.e., $\mathbf{p}_{ss',\text{va}}^{(j)} = h_{\text{va}}(\mathbf{p}_{s,\text{mva}}, \mathbf{p}_{\text{pa}}^{(j)})$, the likelihood function related to the single-bounce propagation path agent – surface s with $s \in \mathcal{S}$ – PA j with PMVA pair index $(s, s) \in \mathcal{D}_{S,n}$ can be expressed by $f(\mathbf{z}_{m,n}^{(j)} | \mathbf{p}_n, \mathbf{p}_{s,\text{mva}})$.

Double-Bounce path likelihood function: Using (5), and (6), and the transformation in (3) twice, i.e., $\mathbf{p}_{ss',\text{va}}^{(j)} = h_{\text{va}}(\mathbf{p}_{s,\text{mva}}, h_{\text{va}}(\mathbf{p}_{s',\text{mva}}, \mathbf{p}_{\text{pa}}^{(j)}))$, the likelihood function related to the double-bounce path agent – surface s with $s \in \mathcal{S}$ – surface s' with $s' \in \mathcal{S}$ – PA j with PMVA pair index $(s, s') \in \mathcal{D}_{D,n}$ can be expressed by $f(\mathbf{z}_{m,n}^{(j)} | \mathbf{p}_n, \mathbf{p}_{s,\text{mva}}, \mathbf{p}_{s',\text{mva}})$. Note that with the proposed MVA-based measurement model, at time n , the measurements collected by all PAs $j \in \{1, \dots, J\}$ can provide information on the same MVA and agent positions $\mathbf{p}_{s,\text{mva}}$, $s \in \mathcal{S}$ and \mathbf{p}_n , respectively.

It is assumed that an MVA generates at most one measurement and that a measurement originates from at most

one MVA. PA j at position $\mathbf{p}_{00,\text{va}}^{(j)} = \mathbf{p}_{\text{pa}}^{(j)}$ with $(0, 0) \in \tilde{\mathcal{D}}_n$ generates a measurements $\mathbf{z}_{m,n}^{(j)}$ with detection probability $p_d(\mathbf{p}_n)$. If MVA s exists ($r_{s,n} = 1$), it generates a MVA-originated measurements $\mathbf{z}_{m,n}^{(j)}$ with detection probability $p_d(\mathbf{p}_n, \mathbf{p}_{s,\text{mva}}) \triangleq p_d(\mathbf{p}_n, h_{\text{va}}(\mathbf{p}_{s,\text{mva}}, \mathbf{p}_{\text{pa}}^{(j)}))$. Note that the detection probability $p_d(\mathbf{p}_n, \mathbf{p}_{s,\text{mva}})$ is related to the SNR of the measurement [4] as well as the availability check of a single-bounce path between the agent position \mathbf{p}_n and the VA position $\mathbf{p}_{ss',\text{va}}^{(j)}$ with $(s, s) \in \mathcal{D}_{S,n}$. The same holds for the double-bounce path between the agent position \mathbf{p}_n and the VA position $\mathbf{p}_{ss',\text{va}}^{(j)}$ with $(s, s') \in \mathcal{D}_{D,n}$ with detection probability $p_d(\mathbf{p}_n, \mathbf{p}_{s,\text{mva}}, \mathbf{p}_{s',\text{mva}}) \triangleq p_d(\mathbf{p}_n, h_{\text{va}}(\mathbf{p}_{s,\text{mva}}, h_{\text{va}}(\mathbf{p}_{s',\text{mva}}, \mathbf{p}_{\text{pa}}^{(j)})))$. A measurement $\mathbf{z}_{m,n}^{(j)}$ may also not originate from any MVA. This type of measurement is referred to as a false positive and is modeled as Poisson point process with mean μ_{fp} and PDF $f_{\text{fp}}(\mathbf{z}_{m,n}^{(j)})$.

Newly detected MVAs, i.e., MVAs that generated a measurement for the first time, are modeled by a Poisson point process with mean μ_n and PDF $f_n(\mathbf{p}_{m,\text{mva}} | \mathbf{p}_n)$. Newly detected MVAs are represented by *new PMVA states* $\bar{\mathbf{y}}_{n,m}^{(j)}$, $m \in \{1, \dots, M_n^{(j)}\}$ in our statistical model [3], [36]. Each new PMVA state corresponds to a measurement $\mathbf{z}_{m,n}^{(j)}$; $\bar{r}_{m,n} = 1$ implies that measurement $\mathbf{z}_{m,n}^{(j)}$ was generated by a newly detected MVA. All new PMVA states are introduced assuming that the corresponding measurements originate from a single-bounce path. This assumption leads to a simpler statistical model and is motivated by the fact that, since double-bounce paths provide a lower SNR than single-bounce paths, new surfaces are typically detected first via a single-bounce measurement.

We also introduce by $\bar{\mathbf{y}}_n^{(j)} \triangleq [\bar{\mathbf{y}}_{1,n}^{(j)T} \dots \bar{\mathbf{y}}_{M_n^{(j)},n}^{(j)T}]^T$ the joint vector of all new PMVA states related to measurements. Introducing new PMVA for each extracted measurement leads to several PMVA states that would grow with time n . Thus, to keep the proposed SLAM algorithm feasible, a sub-optimum pruning step is performed, removing PMVAs with a low probability of existence; this will be further discussed in Sec. IV-A.

B. Legacy PMVAs and State Transition

At time n , measurements are incorporated sequentially across PAs $j \in \{1, \dots, J\}$. Previously detected MVAs, i.e., MVAs that have been detected either at a previous time $n' < n$ or at the current time n but at a previous PA $j' < j$, are represented by legacy PMVA states $\mathbf{y}_{-s,n}^{(j)}$. New PMVAs become legacy PMVAs when the next measurements—either of the next PA or at the next time instance—are taken into account. In particular, the MVA represented by the new MVA state $\bar{\mathbf{y}}_{m',n'}^{(j)}$ introduced due to measurement m' of PA j' at time $n' \leq n$ is represented by the legacy PMVA state $\mathbf{y}_{-s,n}^{(j)}$ at time n , with $s = S_{n'-1} + \sum_{j''=1}^{j'-1} M_n^{(j'')T} + m'$. The number of legacy PMVA at time n , when the measurements of the next PA j are incorporated, is updated according to $S_n^{(j)} = S_n^{(j-1)} + M_n^{(j-1)}$, where $S_n^{(1)} = S_{n-1}$. Here, $S_n^{(j)}$ is equal to the number of all measurements collected up to time n and PA $j-1$. The vector of all legacy PMVA states at time n and up to PA j can now be written as $\mathbf{y}_n^{(j)} = [\mathbf{y}_{-n}^{(j-1)T} \bar{\mathbf{y}}_n^{(j-1)T}]^T$.

³Note that these measurements represent the MPC parameters. For details see [2], [4], [20].

Let us denote by $\mathbf{y}_n^{(1)} \triangleq [\mathbf{y}_{1,n}^T \cdots \mathbf{y}_{S_{n-1},n}^T]^T$, the vector of all legacy PMVA states before any measurements at time n have been incorporated. After the measurements of all PAs $j \in \{1, \dots, J\}$ have been incorporated at time n , the total number of PMVA states is

$$S_n = S_{n-1} + \sum_{j=1}^J M_n^{(j)} = S_n^{(J)} + M_n^{(J)} \quad (7)$$

and the vector of all PMVA states at time n is given by $\mathbf{y}_n = [\mathbf{y}_n^{(J)T} \bar{\mathbf{y}}_n^{(J)T}]^T$.⁴ Legacy PMVAs states $\mathbf{y}_{s,n}$ and the agent state \mathbf{x}_n are assumed to evolve independently across time according to state-transition PDFs $f(\mathbf{y}_{s,n} | \mathbf{y}_{s,n-1})$ and $f(\mathbf{x}_n | \mathbf{x}_{n-1})$, respectively. If PMVA k exists at time $n-1$, i.e., $r_{s,n-1} = 1$, it either disappears, i.e., $\bar{r}_{s,n} = 0$, or survives, i.e., $\bar{r}_{s,n} = 1$; in the latter case, it becomes a legacy PMVA at time n . The probability of survival is denoted by p_s . Suppose the PMVA survives. In that case, its position remains unchanged, i.e., the state-transition pdf of the MVA positions $\mathbf{p}_{s,\text{mva}}$ is given by $f(\mathbf{p}_{s,\text{mva}} | \mathbf{p}_{s,\text{mva}}) = \delta(\mathbf{p}_{s,\text{mva}} - \mathbf{p}_{s,\text{mva}})$. Therefore, $f(\mathbf{p}_{s,\text{mva}}, r_{s,n} | \mathbf{p}_{s,\text{mva}}, r_{s,n-1})$ for $r_{s,n-1} = 1$ is obtained as

$$\begin{aligned} f(\mathbf{p}_{s,\text{mva}}, r_{s,n} | \mathbf{p}_{s,\text{mva}}, r_{s,n-1} = 1) \\ = \begin{cases} (1-p_s) f_D(\mathbf{p}_{s,\text{mva}}), & r_{s,n} = 0 \\ p_s \delta(\mathbf{p}_{s,\text{mva}} - \mathbf{p}_{s,\text{mva}}), & r_{s,n} = 1. \end{cases} \end{aligned} \quad (8)$$

If MVA s does not exist at time $n-1$, i.e., $r_{s,n-1} = 0$, it cannot exist as a legacy PMVA at time n either, thus we get

$$\begin{aligned} f(\mathbf{p}_{s,\text{mva}}, r_{s,n} | \mathbf{p}_{s,\text{mva}}, r_{s,n-1} = 0) \\ = \begin{cases} f_D(\mathbf{p}_{s,\text{mva}}), & r_{s,n} = 0 \\ 0, & r_{s,n} = 1. \end{cases} \end{aligned} \quad (9)$$

For $j \geq 2$, we also define $f^{(j)}(\mathbf{y}_{s,n}^{(j)} | \mathbf{y}_{s,n}^{(j-1)})$ as

$$\begin{aligned} f^{(j)}(\mathbf{p}_{s,\text{mva}}^{(j)}, r_{s,n}^{(j)} | \mathbf{p}_{s,\text{mva}}^{(j-1)}, r_{s,n}^{(j-1)} = 1) \\ = \begin{cases} f_D(\mathbf{p}_{s,\text{mva}}^{(j-1)}), & r_{s,n}^{(j)} = 0 \\ \delta(\mathbf{p}_{s,\text{mva}}^{(j)} - \mathbf{p}_{s,\text{mva}}^{(j-1)}), & r_{s,n}^{(j)} = 1 \end{cases} \end{aligned} \quad (10)$$

and

$$\begin{aligned} f^{(j)}(\mathbf{p}_{s,\text{mva}}^{(j)}, r_{s,n}^{(j)} | \mathbf{p}_{s,\text{mva}}^{(j-1)}, r_{s,n}^{(j-1)} = 0) \\ = \begin{cases} f_D(\mathbf{p}_{s,\text{mva}}^{(j)}), & r_{s,n}^{(j)} = 0 \\ 0, & r_{s,n}^{(j)} = 1. \end{cases} \end{aligned} \quad (11)$$

It is assumed that at time $n=0$ the initial prior PDF $f(\mathbf{y}_{s,0})$, $s = \{1, \dots, S_0\}$ and $f(\mathbf{x}_0)$ are known. All (legacy and new) PMVA states and all agent states up to time n are denoted as $\mathbf{y}_{0:n} \triangleq [\mathbf{y}_0^T \cdots \mathbf{y}_n^T]^T$ and $\mathbf{x}_{0:n} \triangleq [\mathbf{x}_0^T \cdots \mathbf{x}_n^T]^T$, respectively.

C. Data Association Uncertainty

Mapping of reflective surfaces modeled by MVA is complicated by the data association uncertainty: at time n it is

⁴Note that this sequential incorporation of new PMVA states is based on the multisensor multitarget tracking approach introduced in [36, Sec. VIII].

unknown which measurement $\mathbf{z}_{m,n}^{(j)}$ extracted at PA j originated from PA j itself $(0,0)$, from which MVA $(s,s) \in \mathcal{D}_{s,n}^{(j)}$, or from which MVA-MVA pair $(s,s') \in \mathcal{D}_{D,n}^{(j)}$ associated with single-bounce and double-bounce path. Any PMVA-to-measurement association (which considers associations to single PMVAs and PMVA-PMVA pairs as well as to PA j itself) is described by *PMVA-oriented association variables*

$$\mathbf{a}_{ss',n}^{(j)} \triangleq \begin{cases} m \in \mathcal{M}_n^{(j)}, & \text{if legacy PMVA } ss' \text{ generates} \\ & \text{measurement } m \\ 0, & \text{if legacy PMVA } ss' \text{ does not} \\ & \text{generate any measurement} \end{cases} \quad (12)$$

with $(s,s') \in \tilde{\mathcal{D}}_n^{(j)}$ and stacked into the PMVA-oriented association vector as $\mathbf{a}_n^{(j)} = [\mathbf{a}_{00,n}^{(j)} \mathbf{a}_{11,n}^{(j)} \cdots \mathbf{a}_{S_n^{(j)} S_n^{(j)},n}^{(j)}]^T$. To reduce computation complexity, following [3], [35]–[39], we use a redundant description of PMVA-measurement associations, i.e., we introduce *measurement-oriented association variables*

$$\bar{\mathbf{a}}_{m,n}^{(j)} \triangleq \begin{cases} (s,s') \in \tilde{\mathcal{D}}_n^{(j)}, & \text{if measurement } m \text{ is originated} \\ & \text{by legacy PMVA } ss' \\ 0, & \text{if measurement } m \text{ is not gener-} \\ & \text{ated by any legacy PMVA } ss' \end{cases} \quad (13)$$

and stacked into the measurement-oriented association vector as $\bar{\mathbf{a}}_n^{(j)} = [\bar{\mathbf{a}}_{1,n}^{(j)} \cdots \bar{\mathbf{a}}_{M_n^{(j)},n}^{(j)}]^T$. Note that any data association event that can be expressed by both a joint PMVA-oriented association vector $\mathbf{a}_n^{(j)}$ and measurement-oriented association vector $\bar{\mathbf{a}}_n^{(j)}$ is a valid event in the sense that an PMVA generates at most one measurement. A measurement is originated by at most one PMVA. This hybrid representation of data association makes it possible to develop scalable SPAs for simultaneous agents localization and MVA detection, and tracking [3], [35], [36], [39]. Finally, we also introduce the joint association vectors $\mathbf{a}_n = [\mathbf{a}_n^{(1)T} \cdots \mathbf{a}_n^{(J)T}]^T$, $\bar{\mathbf{a}}_n = [\bar{\mathbf{a}}_n^{(1)T} \cdots \bar{\mathbf{a}}_n^{(J)T}]^T$, $\mathbf{a}_{1:n} = [\mathbf{a}_1^T \cdots \mathbf{a}_n^T]^T$, and $\bar{\mathbf{a}}_{1:n} = [\bar{\mathbf{a}}_1^T \cdots \bar{\mathbf{a}}_n^T]^T$.

D. Detection Probability and Availability of Paths

The availability check is performed by establishing a ray [32], [40] between the agent at position \mathbf{p}_n and a VA at position $\mathbf{p}_{ss',\text{va}}^{(j)}$ with $(s,s') \in \tilde{\mathcal{D}}_n^{(j)}$ and check if it intersects with a reflective surface s'' generated by PMVA $s'' \in \mathcal{S}_n \setminus \{s,s'\}$ at position $\mathbf{p}_{s'',\text{mva}}^{(j)}$ and PA j at position $\mathbf{p}_{\text{pa}}^{(j)}$. This availability check is directly integrated into the LOS path detection probability $p_d(\mathbf{p}_n)$ of PA j , the single-bounce detection probabilities $p_d(\mathbf{p}_n, \mathbf{p}_{s,\text{mva}}^{(j)})$ and the double-bounce detection probabilities $p_d(\mathbf{p}_n, \mathbf{p}_{s,\text{mva}}^{(j)}, \mathbf{p}_{s',\text{mva}}^{(j)})$, respectively, given by

$$p_d(\mathbf{p}_n) \triangleq \begin{cases} p_{d,00,n}^{(j)}, & \text{path from agent at } \mathbf{p}_n \text{ to} \\ & \text{VA at } \mathbf{p}_{\text{pa}}^{(j)} \text{ is available} \\ 0, & \text{path is not available} \end{cases} \quad (14)$$

with $(0,0)$,

$$p_d(\mathbf{p}_n, \mathbf{p}_{s,\text{mva}}^{(j)}) \triangleq \begin{cases} p_{d,ss,n}^{(j)}, & \text{path from agent at } \mathbf{p}_n \text{ to} \\ & \text{VA at } \mathbf{p}_{s,\text{va}}^{(j)} \text{ is available} \\ 0, & \text{path is not available} \end{cases} \quad (15)$$

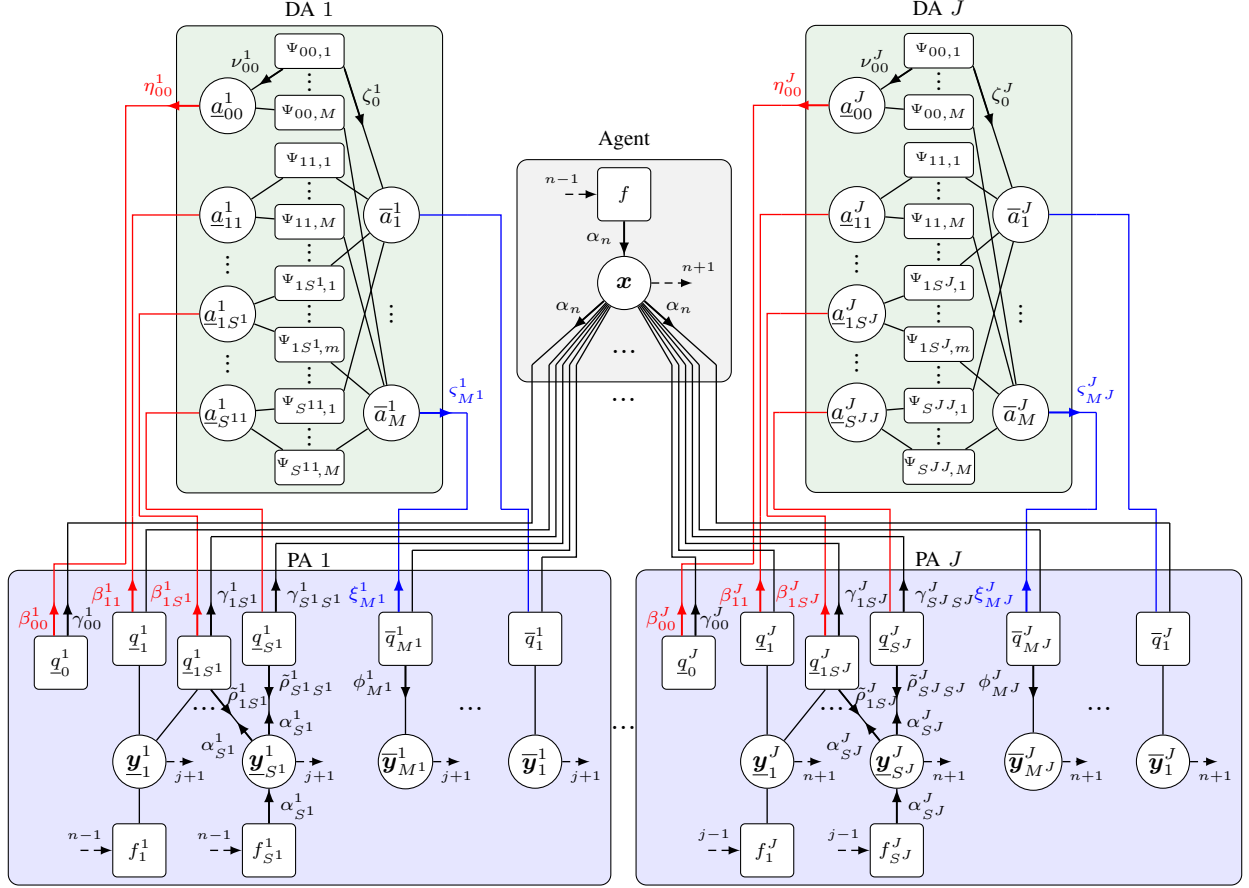


Fig. 3. Factor graph representation of the factorized joint posterior PDF (17). The following short notations are used: $S^1 \triangleq S_{n-1}$, $S^j \triangleq S_n^{(j)}$, $(\cdot)_{Sjj} \triangleq (\cdot)_{S_n^{(j)} S_n^{(j)}}$, $M^j \triangleq M_n^{(j)}$, $\mathbf{y}_s^j \triangleq \mathbf{y}_{s,n}^{(j)}$, $\bar{\mathbf{y}}_m^j \triangleq \bar{\mathbf{y}}_{m,n}^{(j)}$, $\mathbf{q}_0^j \triangleq \mathbf{q}_P(\mathbf{x}_n, \mathbf{a}_{00,n}^{(j)}; \mathbf{z}_n^{(j)})$, $\mathbf{q}_s^j \triangleq \mathbf{q}_S(\mathbf{y}_{s,n}^{(j)}, \mathbf{a}_{ss,n}^{(j)}; \mathbf{x}_n; \mathbf{z}_n^{(j)})$, $\mathbf{q}_{ss'}^j \triangleq \mathbf{q}_D(\mathbf{y}_{s,n}^{(j)}, \mathbf{y}_{s',n}^{(j)}, \mathbf{a}_{ss',n}^{(j)}; \mathbf{x}_n; \mathbf{z}_n^{(j)})$, $\bar{\mathbf{q}}_m^j \triangleq \bar{\mathbf{q}}_S(\bar{\mathbf{y}}_{m,n}^{(j)}, \bar{\mathbf{a}}_{m,n}^{(j)}; \mathbf{x}_n; \mathbf{z}_{m,n}^{(j)})$, $f \triangleq f(\mathbf{x}_n | \mathbf{x}_{n-1})$, $f_s^j \triangleq f(\mathbf{y}_{s,n}^{(j)} | \mathbf{y}_{s,n-1}^{(j)})$, $f_{s'}^j \triangleq f(\mathbf{y}_{s',n}^{(j)} | \mathbf{y}_{s',n-1}^{(j)})$, $\alpha_n = \alpha(\mathbf{x}_n)$, $\alpha_s^j = \alpha_s(\mathbf{y}_{s,n}^{(j)})$, $\beta_{ss'}^j = \beta_{ss'}(\mathbf{a}_{ss',n}^{(j)})$, $\gamma_{ss'}^j = \gamma_{ss'}(\mathbf{x}_n)$, $\xi_m^j = \xi(\bar{\mathbf{a}}_{m,n}^{(j)})$, $\eta_{ss'}^j = \eta(\mathbf{a}_{ss',n}^{(j)})$, $\nu_{ss'}^j = \nu_{m \rightarrow ss'}^{(p)}(\mathbf{a}_{ss',n}^{(j)})$, $\varsigma_m^j = \varsigma(\bar{\mathbf{a}}_{m,n}^{(j)})$, $\varsigma_m^j = \varsigma_{ss' \rightarrow m}^{(p)}(\bar{\mathbf{a}}_{m,n}^{(j)})$, $\tilde{\rho}_{ss'}^j = \rho_{ss'}(\mathbf{y}_{s,n}^{(j)})$, and $\phi_m^j = \phi(\bar{\mathbf{y}}_m^{(j)})$. The dashed lines with arrows indicate messages representing the agent and PMVAs beliefs of time $n-1$, $n+1$ or of anchors $j-1$, $j+1$.

with $(s, s) \in \mathcal{D}_{S,n}^{(j)}$ as well as

$$p_d(\mathbf{p}_n, \mathbf{p}_{s,\text{mva}}^{(j)}, \mathbf{p}_{s',\text{mva}}^{(j)}) \triangleq \begin{cases} p_{d,ss',n}^{(j)}, & \text{path from agent at } \mathbf{p}_n \text{ to} \\ & \text{PMVA at } \mathbf{p}_{s',\text{va}}^{(j)} \text{ is available} \\ 0, & \text{path is not available} \end{cases} \quad (16)$$

with $(s, s') \in \mathcal{D}_{D,n}^{(j)}$.

IV. PROBLEM FORMULATION AND PROPOSED METHOD

In this section, we formulate the detection and estimation problem of interest and present the joint posterior PDF and factor graph underlying the proposed SLAM method.

A. Detection of MVAs and State Estimation

At each time n , a channel estimator [20]–[24] (pre-estimation stage) provides $M_n^{(j)}$ distance estimates $z_{dm,n}^{(j)}$ and AOA estimates $z_{\varphi_{m,n}^{(j)}}$ of MPCs extracted from the radio signal received at PA j . The measurements are stacked into the vector $\mathbf{z}_{m,n}^{(j)} = [z_{dm,n}^{(j)} z_{\varphi_{m,n}^{(j)}}]^T$ with $m \in \mathcal{M}_n^{(j)} \triangleq \{1, \dots, M_n^{(j)}\}$ for PA j and collected in the joint measurement vectors denoted

as $\mathbf{z}_n^{(j)} \triangleq [\mathbf{z}_{1,n}^{(j)T} \dots \mathbf{z}_{M_n^{(j)},n}^{(j)T}]^T$, $\mathbf{z}_n \triangleq [\mathbf{z}_n^{(1)T} \dots \mathbf{z}_n^{(J)T}]^T$, and $\mathbf{z}_{1:n} \triangleq [\mathbf{z}_1^T \dots \mathbf{z}_n^T]^T$.

We aim to estimate the agent state \mathbf{x}_n using all available measurements $\mathbf{z}_{1:n}$ from all PAs up to time n . In particular, we calculate an estimate $\hat{\mathbf{x}}_n$ by using the minimum mean-square error (MMSE) estimator [41, Ch. 4]

$$\hat{\mathbf{x}}_n \triangleq \int \mathbf{x}_n f(\mathbf{x}_n | \mathbf{z}_{1:n}) d\mathbf{x}_n. \quad (18)$$

The map of the environment is represented by reflective surfaces described by PMVAs. Therefore, the positions $\mathbf{p}_{s,\text{mva}}$ of the detected PMVAs $s \in \{1, \dots, S_n\}$ must be estimated. This relies on the marginal posterior existence probabilities $p(r_{s,n} = 1 | \mathbf{z}_{1:n}) = \int f(\mathbf{p}_{s,\text{mva}}, r_{s,n} = 1 | \mathbf{z}_{1:n}) d\mathbf{p}_{s,\text{mva}}$ and the marginal posterior PDFs $f(\mathbf{p}_{s,\text{mva}} | r_{s,n} = 1, \mathbf{z}_{1:n}) = f(\mathbf{p}_{s,\text{mva}}, r_{s,n} = 1 | \mathbf{z}_{1:n}) / p(r_{s,n} = 1 | \mathbf{z}_{1:n})$. A PMVA k is declared to exist if $p(r_{s,n} = 1 | \mathbf{z}_{1:n}) > p_{\text{de}}$, where p_{de} is a detection threshold [41, Ch. 2]. The number \hat{K}_n of PMVA states that are considered to exist is the estimate of the total number K of MVAs. For existing PMVAs, an estimate of its position $\mathbf{p}_{s,\text{mva}}$ can again be calculated by the MMSE [41, Ch. 4]

$$\hat{\mathbf{p}}_{k,\text{mva}} \triangleq \int \mathbf{p}_{k,\text{mva}} f(\mathbf{p}_{k,\text{mva}} | r_{s,n} = 1, \mathbf{z}_{1:n}) d\mathbf{p}_{k,\text{mva}}. \quad (19)$$

$$\begin{aligned}
& f(\mathbf{y}_{0:n}, \mathbf{x}_{0:n}, \mathbf{a}_{1:n}, \bar{\mathbf{a}}_{1:n} | \mathbf{z}_{1:n}) \\
& \propto \underbrace{\left(f(\mathbf{x}_0) \prod_{l=1}^{S_0} f(\mathbf{y}_{l,0}) \right)}_{\text{PMVA's initial prior PDF}} \underbrace{\prod_{n'=1}^n \underbrace{f(\mathbf{x}_{n'} | \mathbf{x}_{n'-1})}_{\text{Agent's state prediction}} \underbrace{\left(\prod_{j=1}^J \underbrace{q_P(\mathbf{x}_{n'}, \underline{a}_{00,n'}^{(j)}; \mathbf{z}_{n'}^{(j)})}_{\text{PA related factors}} \prod_{m'=1}^{M_{n'}^{(j)}} \Psi(\underline{a}_{00,n'}^{(j)}, \bar{a}_{m',n'}^{(j)}) \right)}_{\text{Legacy PMVA's states prediction}}}_{\text{Legacy PMVA states related factors}} \\
& \times \underbrace{\left(\prod_{j=2}^J \left(\prod_{s'=1}^{S_{n'}^{(j)}} f^{(j)}(\mathbf{y}_{s',n'}^{(j)} | \mathbf{y}_{s',n'}^{(j-1)}) \right) \right)}_{\text{Legacy PMVA states related factors}} \underbrace{\prod_{j=1}^J \left(\prod_{s=1}^{S_{n'}^{(j)}} \underbrace{q_S(\mathbf{y}_{s,n'}^{(j)}, \underline{a}_{ss,n'}^{(j)}, \mathbf{x}_{n'}; \mathbf{z}_{n'}^{(j)})}_{\text{New PMVA states's prior PDFs and related factors}} \prod_{m'=1}^{M_{n'}^{(j)}} \Psi(\underline{a}_{ss,n'}^{(j)}, \bar{a}_{m',n'}^{(j)}) \right)}_{\text{New PMVA states's prior PDFs and related factors}} \\
& \times \underbrace{\prod_{s'=1, s' \neq s}^{S_{n'}^{(j)}} \underbrace{q_D(\mathbf{y}_{s,n'}^{(j)}, \mathbf{y}_{s',n'}^{(j)}, \underline{a}_{ss',n'}^{(j)}, \mathbf{x}_{n'}; \mathbf{z}_{n'}^{(j)})}_{\text{Legacy PMVA states related factors}} \prod_{m'=1}^{M_{n'}^{(j)}} \Psi(\underline{a}_{ss',n'}^{(j)}, \bar{a}_{m',n'}^{(j)})}_{\text{Legacy PMVA states related factors}} \underbrace{\left(\prod_{m=1}^{M_{n'}^{(j)}} \bar{q}_S(\bar{\mathbf{y}}_{m,n'}^{(j)}, \bar{a}_{m,n'}^{(j)}, \mathbf{x}_{n'}; \mathbf{z}_{n'}^{(j)}) \right)}_{\text{New PMVA states's prior PDFs and related factors}} \quad (17)
\end{aligned}$$

The calculation of $f(\mathbf{x}_n | \mathbf{z}_{1:n})$, $p(r_{s,n} = 1 | \mathbf{z})$, and $f(\mathbf{p}_{k,\text{mva}} | r_{s,n} = 1, \mathbf{z}_{1:n})$ from the joint posterior $f(\mathbf{y}_{0:n}, \mathbf{x}_{0:n}, \mathbf{a}_{1:n}, \bar{\mathbf{a}}_{1:n} | \mathbf{z}_{1:n})$ by direct marginalization is not feasible.

By performing sequential message passing using the SPA rules [3], [35], [42], [43] on the factor graph in Fig. 3, approximations (“beliefs”) $\tilde{f}(\mathbf{x}_n)$ and $\tilde{f}_s(\mathbf{y}_{s,n})$ of the marginal posterior pdfs $f(\mathbf{x}_n | \mathbf{z}_{1:n})$, $p(r_{s,n} = 1 | \mathbf{z}_{1:n})$, and $f(\mathbf{p}_{k,\text{mva}} | r_{s,n} = 1, \mathbf{z}_{1:n})$ can be obtained in an efficient way for the agent state as well as all legacy and new PMVAs states $s \in \mathcal{S}_n$.

B. The Factor Graph

By using common assumptions [3], [36], and for fixed measurements $\mathbf{z}_{1:n}$, it can be shown that the joint posterior PDF of $\mathbf{y}_{0:n}$, $\mathbf{x}_{0:n}$, $\mathbf{a}_{1:n}$, and $\bar{\mathbf{a}}_{1:n}$, conditioned on $\mathbf{z}_{1:n}$ is given by (17) as shown on top of the page, where we introduced the functions $q_P(\mathbf{x}_{n'}, \underline{a}_{00,n'}^{(j)}; \mathbf{z}_{n'}^{(j)})$, $q_S(\mathbf{y}_{s,n}^{(j)}, \underline{a}_{ss,n}^{(j)}, \mathbf{x}_n; \mathbf{z}_n^{(j)})$, $q_D(\mathbf{y}_{s,n}^{(j)}, \mathbf{y}_{s',n}^{(j)}, \underline{a}_{ss',n}^{(j)}, \mathbf{x}_n; \mathbf{z}_n^{(j)})$, $\bar{q}_S(\bar{\mathbf{y}}_{m,n}^{(j)}, \bar{a}_{m,n}^{(j)}, \mathbf{x}_n; \mathbf{z}_n^{(j)})$, $\bar{f}(\bar{\mathbf{y}}_{s,n})$, and $\Psi(\underline{a}_{s,n}^{(j)}, \bar{a}_{m,n}^{(j)})$ that will be discussed next.

The *pseudo likelihood functions* of PA j $q_P(\mathbf{x}_n, \underline{a}_{00,n}^{(j)}; \mathbf{z}_n^{(j)})$, of legacy PMVAs related to single-bounce paths $q_S(\mathbf{y}_{s,n}^{(j)}, \underline{a}_{ss,n}^{(j)}, \mathbf{x}_n; \mathbf{z}_n^{(j)}) = q_S(\mathbf{p}_{s,\text{mva}}^{(j)}, \underline{r}_{s,n}^{(j)}, \underline{a}_{ss,n}^{(j)}, \mathbf{x}_n; \mathbf{z}_n^{(j)})$ and to double-bounce paths $q_D(\mathbf{y}_{s,n}^{(j)}, \mathbf{y}_{s',n}^{(j)}, \underline{a}_{ss',n}^{(j)}, \mathbf{x}_n; \mathbf{z}_n^{(j)}) = q_D(\mathbf{p}_{s,\text{mva}}^{(j)}, \underline{r}_{s,n}^{(j)}, \mathbf{p}_{s',\text{mva}}^{(j)}, \underline{r}_{s',n}^{(j)}, \underline{a}_{ss',n}^{(j)}, \mathbf{x}_n; \mathbf{z}_n^{(j)})$ are, respectively, given for $(0, 0)$ by

$$\begin{aligned}
& q_P(\mathbf{x}_n, \underline{a}_{00,n}^{(j)}; \mathbf{z}_n^{(j)}) \\
& \triangleq \begin{cases} \frac{p_d(\mathbf{p}_n) f(\mathbf{z}_{m,n}^{(j)} | \mathbf{p}_n)}{\mu_{\text{fp}} f_{\text{fp}}(\mathbf{z}_{m,n}^{(j)})}, & \underline{a}_{00,n}^{(j)} = m \in \mathcal{M}_n^{(j)} \\ 1 - p_d(\mathbf{p}_n), & \underline{a}_{00,n}^{(j)} = 0 \end{cases} \quad (20)
\end{aligned}$$

for $(s, s) \in \mathcal{D}_{S,n}^{(j)}$ by

$$\begin{aligned}
& q_S(\mathbf{p}_{s,\text{mva}}^{(j)}, \underline{r}_{s,n}^{(j)} = 1, \underline{a}_{ss,n}^{(j)}, \mathbf{x}_n; \mathbf{z}_n^{(j)}) \\
& \triangleq \begin{cases} \frac{p_d(\mathbf{p}_n, \mathbf{p}_{s,\text{mva}}) f(\mathbf{z}_{m,n}^{(j)} | \mathbf{p}_n, \mathbf{p}_{s,\text{mva}})}{\mu_{\text{fp}} f_{\text{fp}}(\mathbf{z}_{m,n}^{(j)})}, & \underline{a}_{ss,n}^{(j)} = m \in \mathcal{M}_n^{(j)} \\ 1 - p_d(\mathbf{p}_n, \mathbf{p}_{s,\text{mva}}), & \underline{a}_{ss,n}^{(j)} = 0 \end{cases} \quad (21)
\end{aligned}$$

and $q_S(\mathbf{p}_{s,\text{mva}}^{(j)}, \underline{r}_{s,n}^{(j)} = 0, \underline{a}_{ss,n}^{(j)}, \mathbf{x}_n; \mathbf{z}_n^{(j)}) \triangleq \delta(\underline{a}_{ss,n}^{(j)})$ as well as for $(s, s') \in \mathcal{D}_{D,n}^{(j)}$ by

$$\begin{aligned}
& q_D(\mathbf{p}_{s,\text{mva}}^{(j)}, \underline{r}_{s,n}^{(j)} = 1, \mathbf{p}_{s',\text{mva}}^{(j)}, \underline{r}_{s',n}^{(j)} = 1, \underline{a}_{ss',n}^{(j)}, \mathbf{x}_n; \mathbf{z}_n^{(j)}) \\
& \triangleq \begin{cases} \frac{p_d(\mathbf{p}_n, \mathbf{p}_{s,\text{mva}}, \mathbf{p}_{s',\text{mva}})}{\mu_{\text{fp}}} \\ \times \frac{f(\mathbf{z}_{m,n}^{(j)} | \mathbf{p}_n, \mathbf{p}_{s,\text{mva}}, \mathbf{p}_{s',\text{mva}})}{f_{\text{fp}}(\mathbf{z}_{m,n}^{(j)})}, & \underline{a}_{ss'}^{(j)} = m \in \mathcal{M}_n^{(j)} \\ 1 - p_d(\mathbf{p}_n, \mathbf{p}_{s,\text{mva}}, \mathbf{p}_{s',\text{mva}}), & \underline{a}_{ss'}^{(j)} = 0 \end{cases} \quad (22)
\end{aligned}$$

and $q_D(\mathbf{p}_{s,\text{mva}}^{(j)}, \underline{r}_{s,n}^{(j)}, \mathbf{p}_{s',\text{mva}}^{(j)}, \underline{r}_{s',n}^{(j)}, \underline{a}_{ss',n}^{(j)}, \mathbf{x}_n; \mathbf{z}_n^{(j)}) \triangleq \delta(\underline{a}_{ss',n}^{(j)})$ if any $\underline{r}_{s'',n}^{(j)} = 0$ for $s'' \in \{s, s'\}$.

The *pseudo likelihood functions* related to new PMVAs $\bar{q}_S(\bar{\mathbf{y}}_{m,\text{mva}}^{(j)}, \bar{a}_{m,n}^{(j)}, \mathbf{x}_n; \mathbf{z}_n^{(j)}) = \bar{q}_S(\bar{\mathbf{p}}_{m,\text{mva}}^{(j)}, \bar{r}_{s,n}^{(j)}, \bar{a}_{m,n}^{(j)}, \mathbf{x}_n; \mathbf{z}_n^{(j)})$ is given by

$$\begin{aligned}
& \bar{q}_S(\bar{\mathbf{p}}_{m,\text{mva}}^{(j)}, \bar{r}_{s,n}^{(j)} = 1, \bar{a}_{m,n}^{(j)}, \mathbf{x}_n; \mathbf{z}_n^{(j)}) \\
& \triangleq \begin{cases} 0, & \bar{a}_{m,n}^{(j)} \in \tilde{\mathcal{D}}_n^{(j)} \\ \frac{\mu_n f_n(\bar{\mathbf{p}}_{m,\text{mva}}^{(j)} | \mathbf{p}_n) f(\mathbf{z}_{m,n}^{(j)} | \mathbf{p}_n, \bar{\mathbf{p}}_{m,\text{mva}}^{(j)})}{\mu_{\text{fp}} f_{\text{fp}}(\mathbf{z}_{m,n}^{(j)})}, & \bar{a}_{m,n}^{(j)} = 0 \end{cases} \quad (23)
\end{aligned}$$

and $\bar{q}_S(\bar{\mathbf{p}}_{m,\text{mva}}^{(j)}, \bar{r}_{s,n}^{(j)} = 0, \bar{a}_{m,n}^{(j)}, \mathbf{x}_n; \mathbf{z}_n^{(j)}) \triangleq 1$, respectively. Note that the first line in (23) is zero because per definition, the new PMVA with index m exists ($\bar{r}_{m,n} = 1$) if and only if the measurement is not associated to a legacy PMVA. For $\bar{a}_{m,n}^{(j)} = 0$, for each measurement $\mathbf{z}_{m,n}^{(j)}$ a new PMVA is introduced, implying that each measurement $\mathbf{z}_{m,n}^{(j)}$ is assumed to originate from a single-bounce path corresponding to exactly one PMVA $s \in \mathcal{M}_n^{(j)}$ (not a pair of PMVAs).

Finally, the binary *indicator functions* that check consistency for any pair $(\underline{a}_{ss',n}^{(j)}, \bar{a}_{m,n}^{(j)})$ of PMVA-oriented and measurement-oriented association variable at time n , read

$$\begin{aligned}
& \Psi(\underline{a}_{ss',n}^{(j)}, \bar{a}_{m,n}^{(j)}) \\
& \triangleq \begin{cases} 0, & \underline{a}_{ss',n}^{(j)} = m, \bar{a}_{m,n}^{(j)} \neq ss' \text{ or } \underline{a}_{ss',n}^{(j)} \neq m, \bar{a}_{m,n}^{(j)} = ss' \\ 1, & \text{otherwise.} \end{cases}
\end{aligned}$$

In case the joint PMVA-oriented association vector \mathbf{a}_n and the measurement-oriented association vector $\bar{\mathbf{a}}_n$ do not describe

the same association event, at least one indicator function in (17) is zero. Thus $f(\mathbf{y}_{0:n}, \mathbf{x}_{0:n}, \mathbf{a}_{1:n}, \bar{\mathbf{a}}_{1:n} | \mathbf{z}_{1:n})$ is zero as well. A detailed derivation of this factor graph is provided in the supplementary material [34, Sec. II]. The factor graph representing factorization (17) is shown in Fig. 3.

V. PROPOSED SUM-PRODUCT ALGORITHM

Since our factor graph in Fig. 3 has cycles, we have to decide on a specific order of message computation [42], [44]. We choose the order according to the following rules: (i) messages are only sent forward in time⁵; (ii) messages are only sent from PA $j-1$ to PA j , i.e., the measurements of PA are processed serial, thus, PA $j-1$ establishes new PMVAs that are acting as legacy PMVAs for PA j ; (iii) *iterative* message passing is only performed for data association [3], [4], i.e., in particular, for the loops connecting different PMVAs, we only perform a single message passing iteration; and (iv) along an edge connecting an agent state variable node and a new PMVA state variable node, messages are only sent from the former to the latter. With these rules, the message passing equations of the SPA [42] yield the following operations at each time step. The corresponding messages are shown in Fig. 3.

We note that similarly to the “dummy PDFs” introduced in Section III, we consider messages $\varphi(\mathbf{y}_{k,n}^{(j)}) = \varphi(\mathbf{a}_{k,n}^{(j)}, r_{k,n}^{(j)})$ for non-existing PMVA states, i.e., for $r_{k,n}^{(j)} = 0$. We define these messages by $\varphi(\mathbf{a}_{k,n}^{(j)}, 0) = \varphi_{k,n}^{(j)}$ (note that these messages are not PDFs and thus are not required to integrate to 1). To keep the notation concise, we also define the sets $\mathcal{M}_{0,n}^{(j)} \triangleq \mathcal{M}_n^{(j)} \cup \{0\}$ and $\tilde{\mathcal{D}}_{0,n}^{(j)} \in \tilde{\mathcal{D}}_n^{(j)} \cup \{0\}$.

A. Prediction Step

First, a *prediction step* is performed for the agent and all legacy PMVAs $s \in S_{n-1}$. Based on the SPA rule, the prediction message for the agent state is given by

$$\alpha(\mathbf{x}_n) = \int f(\mathbf{x}_n | \mathbf{x}_{n-1}) \tilde{f}(\mathbf{x}_{n-1}) d\mathbf{x}_{n-1} \quad (24)$$

and the prediction message for the legacy PMVAs is given by

$$\alpha_s(\mathbf{p}_{s,\text{mva}}, r_{s,n}) = \sum_{r_{k,n-1} \in \{0,1\}} \int f(\mathbf{p}_{s,\text{mva}}, r_{s,n} | \mathbf{p}_{s,\text{mva}}, r_{s,n-1}) \times \tilde{f}(\mathbf{p}_{s,\text{mva}}, r_{s,n-1}) d\mathbf{p}_{s,\text{mva}} \quad (25)$$

$s \in \{1, \dots, S_{n-1}\}$, where the beliefs of the mobile agent state, $\tilde{f}(\mathbf{x}_{n-1})$, and of the PMVA states, $\tilde{f}(\mathbf{p}_{s,\text{mva}}, r_{s,n-1})$, were calculated at the preceding time $n-1$. Inserting (8) and (9) for $f(\mathbf{p}_{s,\text{mva}}, r_{s,n} | \mathbf{p}_{s,\text{mva}}, r_{s,n-1} = 1)$ and $f(\mathbf{p}_{s,\text{mva}}, r_{s,n} | \mathbf{p}_{s,\text{mva}}, r_{s,n-1} = 0)$, respectively, we obtain

$$\alpha_s(\mathbf{p}_{s,\text{mva}}, 1) = p_s \int \delta(\mathbf{p}_{s,\text{mva}} - \mathbf{p}_{s,\text{mva}}) \tilde{f}_s(\mathbf{p}_{s,\text{mva}}, 1) d\mathbf{p}_{s,\text{mva}} \quad (26)$$

and $\alpha_s(\mathbf{p}_{s,\text{mva}}, 0) = \alpha_{s,n} f_D(\mathbf{p}_{s,\text{mva}})$ with

$$\alpha_{s,n} = (1-p_s) \int \tilde{f}_s(\mathbf{p}_{s,\text{mva}}, 1) d\mathbf{p}_{s,\text{mva}} + \tilde{f}_{s,n-1}. \quad (27)$$

⁵This is equivalent to a joint filtering approach with the assumption that the states are conditionally independent given the past measurements.

We note that $\tilde{f}_{s,n-1} \triangleq \int \tilde{f}_s(\mathbf{p}_{s,\text{mva}}, 0) d\mathbf{p}_{s,\text{mva}}$ approximates the probability of non-existence of legacy PMVA s at the previous time step $n-1$.

B. Sequential PA Update

At iteration $j \in \{1, \dots, J\}$, the following operations are calculated for all legacy and new PMVAs.

1) *Transition of New and Legacy PMVA States Between PAs*: For $j = 1$, the number of legacy PMVAs is $S_n^{(1)} = S_{n-1}$ with the corresponding state $\mathbf{y}_n^{(1)} \triangleq [\mathbf{y}_{1,n}^T \dots \mathbf{y}_{S_{n-1},n}^T]^T$. Furthermore, the state $\bar{\mathbf{y}}^{(j-1)}$ is empty and the prediction message of legacy PMVAs is $\alpha_s(\mathbf{p}_{s,\text{mva}}^{(j)}, r_{s,n}) \triangleq \alpha_s(\mathbf{p}_{s,\text{mva}}, r_{s,n})$ as well as $\alpha_{s,n}^{(j)} \triangleq \alpha_{s,n}$. For $j > 1$, we have $S_n^{(j)} = S_n^{(j-1)} + M_n^{(j-1)}$ legacy PMVAs with states $\mathbf{y}_n^{(j)} = [\mathbf{y}_n^{(j-1)T} \bar{\mathbf{y}}_n^{(j-1)T}]^T$ and $M_n^{(j)}$ new PMVAs with states $\bar{\mathbf{y}}_n^{(j)}$. For $1 \leq s \leq S_n^{(j-1)}$, using (10), (11), and (25) the prediction message of former legacy PMVAs is given by

$$\alpha_s(\mathbf{p}_{s,\text{mva}}^{(j)}, 1) = \int \delta(\mathbf{p}_{s,\text{mva}}^{(j)} - \mathbf{p}_{s,\text{mva}}^{(j-1)}) \gamma(\mathbf{p}_{s,\text{mva}}^{(j-1)}, 1) d\mathbf{p}_{s,\text{mva}}^{(j-1)} \quad (28)$$

and $\alpha_s(\mathbf{p}_{s,\text{mva}}^{(j)}, 0) = \alpha_{s,n}^{(j)} f_D(\mathbf{p}_{s,\text{mva}}^{(j)})$ with $\alpha_{s,n}^{(j)} = \gamma_{s,n}^{(j-1)}$. The prediction message of former new PMVAs is $\alpha_s(\mathbf{p}_{s,\text{mva}}^{(j)}, r_{s,n}) \triangleq \phi(\bar{\mathbf{y}}_n^{(j)})$ and $\alpha_{s,n}^{(j)} \triangleq \phi_{s,n}^{(j)}$.

2) *Checking the Availability of Propagation Paths*: The proposed SPA algorithm performs an availability check for each propagation path using *ray-launching* [32], [40] to determine whether a VA can provide map information. First, the VA positions $\mathbf{p}_{ss',\text{va}}^{(j)}$ are determined by applying (3) directly to PA j at position $\mathbf{p}_{\text{pa}}^{(j)}$ to get single-bounce-related VAs at positions $\mathbf{p}_{ss',\text{va}}^{(j)}$. Next, (3) is also applied to this single-bounce-related VAs to get double-bounce-related VAs at positions $\mathbf{p}_{ss',\text{va}}^{(j)}$. A ray between the agent at position \mathbf{p}_n and a VA at position $\mathbf{p}_{ss',\text{va}}^{(j)}$ with $(s, s') \in \mathcal{D}_n^{(j)}$ is then established and a check if it intersects with a reflective surface s'' generated by PMVA $s'' \in \mathcal{S}_n \setminus \{s, s'\}$ at position $\mathbf{p}_{s'',\text{mva}}^{(j)}$ and PA j at position $\mathbf{p}_{\text{pa}}^{(j)}$ is performed based on the fast line intersection algorithm [40]. In case the path between the agent position and a VA position or between two VA positions (double-bounce path) intersects with a reflective surface (e.g., it is blocked), the corresponding path is not available at the agent position \mathbf{p}_n . Hence, the corresponding VA cannot be associated with measurements at time n .

3) *Measurement Evaluation for the LOS Path*: The messages $\beta_{00}(\mathbf{a}_{00,n}^{(j)})$ passed from the factor node $q_P(\mathbf{x}_n, \mathbf{a}_{00,n}^{(j)}; \mathbf{z}_n^{(j)})$ to the feature-oriented association variables $\mathbf{a}_{00,n}^{(j)}$ are calculated as

$$\beta_{00}(\mathbf{a}_{00,n}^{(j)}) = \int \alpha(\mathbf{x}_n) q_P(\mathbf{x}_n, \mathbf{a}_{00,n}^{(j)}; \mathbf{z}_n^{(j)}) d\mathbf{x}_n. \quad (29)$$

4) *Measurement Evaluation for Legacy PMVAs*: For $s = s'$, the messages $\beta_{ss}(\mathbf{a}_{ss,n}^{(j)})$ passed from the factor node $q_S(\mathbf{p}_{s,\text{mva}}^{(j)}, r_{s,n}, \mathbf{a}_{ss,n}^{(j)}; \mathbf{x}_n; \mathbf{z}_n^{(j)})$ of single PMVAs to the feature-oriented association variables $\mathbf{a}_{ss,n}^{(j)}$ given by

$$\beta_{ss}(\mathbf{a}_{ss,n}^{(j)})$$

$$= \iint \alpha_s(\underline{\mathbf{p}}_{s,\text{mva}}^{(j)}, 1) \alpha(\mathbf{x}_n) \underline{q}_S(\underline{\mathbf{p}}_{s,\text{mva}}^{(j)}, \underline{r}_{s,n}^{(j)}, \underline{a}_{ss,n}^{(j)}, \mathbf{x}_n; \mathbf{z}_n^{(j)}) \times d\mathbf{x}_n d\underline{\mathbf{p}}_{s,\text{mva}}^{(j)} + 1(\underline{a}_{ss,n}^{(j)}) \alpha_{s,n}^{(j)}. \quad (30)$$

For $s \neq s'$, the message $\beta_{ss'}(\underline{a}_{ss',n}^{(j)})$ passed from the factor node $\underline{q}_D(\underline{\mathbf{p}}_{s,\text{mva}}^{(j)}, \underline{r}_{s,n}^{(j)}, \underline{\mathbf{p}}_{s',\text{mva}}^{(j)}, \underline{r}_{s',n}^{(j)}, \underline{a}_{ss',n}^{(j)}, \mathbf{x}_n; \mathbf{z}_n^{(j)})$ of pairs of PMVAs to the feature-oriented association variables $\underline{a}_{ss',n}^{(j)}$ are obtained as

$$\beta_{ss'}(\underline{a}_{ss',n}^{(j)}) = \iint \alpha_s(\underline{\mathbf{p}}_{s,\text{mva}}^{(j)}, 1) \alpha_{s'}(\underline{\mathbf{p}}_{s',\text{mva}}^{(j)}, 1) \alpha(\mathbf{x}_n) \times \underline{q}_D(\underline{\mathbf{p}}_{s,\text{mva}}^{(j)}, \underline{r}_{s,n}^{(j)}, \underline{\mathbf{p}}_{s',\text{mva}}^{(j)}, \underline{r}_{s',n}^{(j)}, \underline{a}_{ss',n}^{(j)}, \mathbf{x}_n; \mathbf{z}_n^{(j)}) \times d\mathbf{x}_n d\underline{\mathbf{p}}_{s,\text{mva}}^{(j)} + 1(\underline{a}_{ss',n}^{(j)}) \alpha_{s,n}^{(j)}. \quad (31)$$

5) *Measurement Evaluation for New PMVAs:* For PA j , the messages $\xi(\underline{a}_{m,n}^{(j)})$ sent from the factor node $\bar{q}_S(\underline{\mathbf{p}}_{m,\text{mva}}^{(j)}, \bar{r}_{k,\text{mva}}^{(j)}, \bar{a}_{m,n}^{(j)}, \mathbf{x}_n; \mathbf{z}_{m,n}^{(j)})$ to the variable nodes corresponding to the measurement-oriented association variables $\bar{a}_{m,n}^{(j)}$ are given by

$$\xi(\bar{a}_{m,n}^{(j)}) = \sum_{\bar{r}_{m,n}^{(j)} \in \{0,1\}} \iint \bar{q}_S(\underline{\mathbf{p}}_{m,\text{mva}}^{(j)}, \bar{r}_{k,\text{mva}}^{(j)}, \bar{a}_{m,n}^{(j)}, \mathbf{x}_n; \mathbf{z}_{m,n}^{(j)}) \times \alpha(\mathbf{x}_n) d\mathbf{x}_n d\underline{\mathbf{p}}_{m,\text{mva}}^{(j)}. \quad (32)$$

Using the expression of $\bar{q}_S(\underline{\mathbf{p}}_{m,\text{mva}}^{(j)}, \bar{r}_{k,\text{mva}}^{(j)}, \bar{a}_{m,n}^{(j)}, \mathbf{x}_n; \mathbf{z}_{m,n}^{(j)})$ in Section IV-B in (23), Eq. (32) simplifies to $\xi(\bar{a}_{m,n}^{(j)}) = 1$ for $\bar{a}_{m,n}^{(j)} \in \mathcal{D}_n^{(j)}$, and for $\bar{a}_{m,n}^{(j)} = 0$ it becomes

$$\xi(\bar{a}_{m,n}^{(j)}) = 1 + \frac{\mu_n}{\mu_{\text{fp}} f_{\text{fp}}(\mathbf{z}_{m,n}^{(j)})} \iint \alpha(\mathbf{x}_n) f_n(\underline{\mathbf{p}}_{m,\text{mva}}^{(j)} | \mathbf{x}_n) \times f(\mathbf{z}_{m,n}^{(j)} | \mathbf{x}_n, \underline{\mathbf{p}}_{m,\text{mva}}^{(j)}) d\mathbf{x}_n d\underline{\mathbf{p}}_{m,\text{mva}}^{(j)}. \quad (33)$$

6) *Iterative Data Association:* Next, from $\beta(\underline{a}_{ss',n}^{(j)})$ and $\xi(\bar{a}_{m,n}^{(j)})$, messages $\eta(\underline{a}_{ss',n}^{(j)})$ and $\varsigma(\bar{a}_{m,n}^{(j)})$ are obtained using loopy (iterative) BP. First, for each measurement, $m \in \mathcal{M}_n^{(j)}$, messages $\nu_{m \rightarrow s}^{(p)}(\underline{a}_{ss',n}^{(j)})$ and $\zeta_{s \rightarrow m}^{(p)}(\bar{a}_{m,n}^{(j)})$ are calculated iteratively according to [36], [39] for $ss' \in \bar{\mathcal{D}}_n^{(j)}$, $m \in \mathcal{M}_n^{(j)}$, and iteration index $p \in \{1, \dots, P\}$. After the last iteration $p = P$, the messages $\eta(\underline{a}_{ss',n}^{(j)})$ and $\varsigma(\bar{a}_{m,n}^{(j)})$ are calculated according to [36], [39]. Details are provided in the supplementary material [34, Sec. III].

7) *Measurement Update for the Agent:* The message $\gamma_{00}^{(j)}(\mathbf{x}_n)$ sent from the factor node $\underline{q}_P(\mathbf{x}_n, \underline{a}_{00,n}^{(j)}; \mathbf{z}_n^{(j)})$ to the agent variable node is computed as

$$\gamma_{00}^{(j)}(\mathbf{x}_n) = \sum_{\underline{a}_{00,n}^{(j)} \in \mathcal{M}_{0,n}^{(j)}} \eta(\underline{a}_{00,n}^{(j)}) \underline{q}_P(\mathbf{x}_n, \underline{a}_{00,n}^{(j)}; \mathbf{z}_n^{(j)}). \quad (34)$$

For $s = s'$, the messages $\gamma_{ss}^{(j)}(\mathbf{x}_n)$ sent from the factor node $\underline{q}_S(\underline{\mathbf{p}}_{s,\text{mva}}^{(j)}, 1, \underline{a}_{ss,n}^{(j)}, \mathbf{x}_n; \mathbf{z}_n^{(j)})$ to the agent variable node are given by

$$\gamma_{ss}^{(j)}(\mathbf{x}_n) = \sum_{\underline{a}_{ss,n}^{(j)} \in \mathcal{M}_{0,n}^{(j)}} \eta(\underline{a}_{ss,n}^{(j)}) \int \underline{q}_S(\underline{\mathbf{p}}_{s,\text{mva}}^{(j)}, 1, \underline{a}_{ss,n}^{(j)}, \mathbf{x}_n; \mathbf{z}_n^{(j)}) \times \alpha_s(\underline{\mathbf{p}}_{s,\text{mva}}^{(j)}, 1) d\underline{\mathbf{p}}_{s,\text{mva}}^{(j)} + \eta(\underline{a}_{ss,n}^{(j)} = 0) \alpha_{s,n}^{(j)}. \quad (35)$$

Furthermore, for $s \neq s'$, the messages passed from the factor node $\underline{q}_D(\underline{\mathbf{p}}_{s,\text{mva}}^{(j)}, 1, \underline{\mathbf{p}}_{s',\text{mva}}^{(j)}, 1, \underline{a}_{ss',n}^{(j)}, \mathbf{x}_n; \mathbf{z}_n^{(j)})$ to the agent variable node are obtained as

$$\gamma_{ss'}^{(j)}(\mathbf{x}_n) = \sum_{\underline{a}_{ss',n}^{(j)} \in \mathcal{M}_{0,n}^{(j)}} \eta(\underline{a}_{ss',n}^{(j)}) \alpha_s(\underline{\mathbf{p}}_{s,\text{mva}}^{(j)}, 1) \alpha_{s'}(\underline{\mathbf{p}}_{s',\text{mva}}^{(j)}, 1) \times \int \underline{q}_D(\underline{\mathbf{p}}_{s,\text{mva}}^{(j)}, 1, \underline{\mathbf{p}}_{s',\text{mva}}^{(j)}, 1, \underline{a}_{ss',n}^{(j)}, \mathbf{x}_n; \mathbf{z}_n^{(j)}) \times d\underline{\mathbf{p}}_{s,\text{mva}}^{(j)} d\underline{\mathbf{p}}_{s',\text{mva}}^{(j)} + \eta(\underline{a}_{ss',n}^{(j)} = 0) \alpha_{s,n}^{(j)} \alpha_{s',n}^{(j)}. \quad (36)$$

8) *Measurement Update for Legacy PMVAs:* Similarly, for $s = s'$, the messages $\rho_{ss'}(\underline{\mathbf{y}}_s^{(j)})$ sent to the legacy PMVAs variable nodes are given by

$$\rho_{ss}(\underline{\mathbf{p}}_{s,\text{mva}}^{(j)}, 1) = \sum_{\underline{a}_{ss,n}^{(j)} \in \mathcal{M}_{0,n}^{(j)}} \int \eta(\underline{a}_{ss,n}^{(j)}) \alpha(\mathbf{x}_n) \times \underline{q}_S(\underline{\mathbf{p}}_{s,\text{mva}}^{(j)}, 1, \underline{a}_{ss,n}^{(j)}, \mathbf{x}_n; \mathbf{z}_n^{(j)}) d\mathbf{x}_n \quad (37)$$

$$\rho_{ss}^{(j)} \triangleq \rho_{ss}(\underline{\mathbf{p}}_{s,\text{mva}}^{(j)}, 0) = \eta(\underline{a}_{ss,n}^{(j)} = 0) \quad (38)$$

and for $s \neq s'$ by

$$\rho_{ss'}(\underline{\mathbf{p}}_{s,\text{mva}}^{(j)}, 1) = \sum_{\underline{a}_{ss',n}^{(j)} \in \mathcal{M}_{0,n}^{(j)}} \int \eta(\underline{a}_{ss',n}^{(j)}) \alpha(\mathbf{x}_n) \alpha_{s'}(\underline{\mathbf{p}}_{s',\text{mva}}^{(j)}, 1) \times \underline{q}_D(\underline{\mathbf{p}}_{s,\text{mva}}^{(j)}, 1, \underline{\mathbf{p}}_{s',\text{mva}}^{(j)}, 1, \underline{a}_{ss',n}^{(j)}, \mathbf{x}_n; \mathbf{z}_n^{(j)}) \times d\mathbf{x}_n d\underline{\mathbf{p}}_{s',\text{mva}}^{(j)} \quad (39)$$

$$\rho_{ss'}^{(j)} \triangleq \rho_{ss'}(\underline{\mathbf{p}}_{s,\text{mva}}^{(j)}, 0) = \eta(\underline{a}_{ss',n}^{(j)} = 0). \quad (40)$$

Based on these messages, the message sent to the next PA $\gamma(\underline{\mathbf{y}}_s^{(j)}) \triangleq \gamma(\underline{\mathbf{p}}_{s,\text{mva}}^{(j)}, \underline{r}_{k,n}^{(j)})$ is computed as

$$\gamma(\underline{\mathbf{p}}_{s,\text{mva}}^{(j)}, 1) = \rho_s(\underline{\mathbf{p}}_{s,\text{mva}}^{(j)}, 1) + \prod_{s'=1, s \neq s'}^{S_n^{(j)}} \rho_{ss'}(\underline{\mathbf{p}}_{s,\text{mva}}^{(j)}, 1) \quad (41)$$

$$\gamma_{s,n}^{(j)} \triangleq \gamma(\underline{\mathbf{p}}_{s,\text{mva}}^{(j)}, 0) = \rho_{ss}^{(j)} + \prod_{s'=1, s \neq s'}^{S_n^{(j)}} \rho_{ss'}^{(j)}. \quad (42)$$

9) *Measurement Update for New PMVAs:* Finally, the messages $\phi(\underline{\mathbf{y}}_s^{(j)}) \triangleq \phi(\underline{\mathbf{p}}_{s,\text{mva}}^{(j)}, \bar{r}_{k,n}^{(j)})$ sent to the new PMVA variable nodes are obtained as

$$\phi(\underline{\mathbf{p}}_{s,\text{mva}}^{(j)}, 1) = \int \bar{q}_S(\underline{\mathbf{p}}_{m,\text{mva}}^{(j)}, 1, \bar{a}_{m,n}^{(j)}, \mathbf{x}_n; \mathbf{z}_{m,n}^{(j)}) \times \alpha(\mathbf{x}_n) d\mathbf{x}_n \varsigma(\bar{a}_{m,n}^{(j)} = 0) \quad (43)$$

$$\phi_{m,n}^{(j)} \triangleq \phi(\underline{\mathbf{p}}_{s,\text{mva}}^{(j)}, 0) = \sum_{\bar{a}_{m,n}^{(j)} \in \bar{\mathcal{D}}_{0,n}^{(j)}} \varsigma(\bar{a}_{m,n}^{(j)}). \quad (44)$$

C. Belief Calculation

After the messages for all PAs, $j \in \{1, \dots, J\}$ are computed, the belief $\tilde{f}(\mathbf{x}_n)$ of the agent state can be calculated as normalized production of all incoming messages [42], i.e.,

$$\tilde{f}(\mathbf{x}_n) = C_n \alpha(\mathbf{x}_n) \prod_{(s,s') \in \bar{\mathcal{D}}_n^{(J)}} \gamma_{ss'}^{(J)}(\mathbf{x}_n) \quad (45)$$

with normalization constant $C_n = (\int \alpha(\mathbf{x}_n) \prod_{(s,s') \in \tilde{\mathcal{D}}_n^{(j)}} \gamma_{ss'}^{(j)}(\mathbf{x}_n) d\mathbf{x}_n)^{-1}$ that guarantees that (45) is a valid probability distribution. Similarly, the beliefs $\tilde{f}_s(\mathbf{y}_{s,n}^{(j)}) = \tilde{f}_s(\mathbf{p}_{s,\text{mva}}^{(j)}, \mathbf{r}_{s,n}^{(j)})$ of legacy PMVA $s \in S_n^J$, is given by

$$\tilde{f}_s(\mathbf{y}_{s,n}^{(j)}) = \underline{C}_{s,n} \gamma(\mathbf{y}_s^{(j)}) \quad (46)$$

with constant $\underline{C}_{s,n} = (\int \gamma(\mathbf{p}_{s,\text{mva}}^{(j)}, \mathbf{r}_{s,n}^{(j)} = 1) d\mathbf{p}_{s,\text{mva}}^{(j)} + \gamma_{s,n}^{(j)})^{-1}$. Similarly, the $\tilde{f}_s(\mathbf{y}_{s,n}^{(j)}) = \tilde{f}_s(\mathbf{p}_{s,\text{mva}}^{(j)}, \mathbf{r}_{s,n}^{(j)})$ of new PMVA $s \in M_n^J$, is obtained as

$$\tilde{f}_s(\mathbf{y}_{s,n}^{(j)}) = \overline{C}_{s,n} \phi(\mathbf{y}_s^{(j)}) \quad (47)$$

where $\overline{C}_{s,n} = (\int \phi(\mathbf{y}_s^{(j)}) d\mathbf{y}_s^{(j)} + \phi_{s,n}^{(j)})^{-1}$ is again a constant.

A computationally feasible sequential particle-based message passing implementation can be obtained along the line with [3], [35], [43]. In particular, we adopted the approach in [43] using the “stacked state” comprising the agent state and the PMVA states. To avoid that the number of PMVA states grows indefinitely, PMVAs states with $p(r_{s,n} = 1 | \mathbf{z}_{1:n})$ below a threshold p_{pr} are removed from the state space (“pruned”) after processing the measurements of each PA j .

VI. SIMULATION RESULTS

The performance of the proposed MVA-based SLAM algorithm is validated and compared with the multipath-based SLAM algorithm from [3]⁶ using synthetic measurements as well as real radio measurements. Additional simulation results can be found in the supplementary material [34, Sec. IV].

A. Common Simulation Setup

The following setups and parameters are commonly used for both synthetic and real measurements. The agent’s state-transition pdf $f(\mathbf{x}_n | \mathbf{x}_{n-1})$, with $\mathbf{x}_n = [\mathbf{p}_n^T \mathbf{v}_n^T]^T$, is defined by a linear, near constant-velocity motion model [45, Sec. 6.3.2], i.e., $\mathbf{x}_n = \mathbf{A}\mathbf{x}_{n-1} + \mathbf{B}\mathbf{w}_n$. Here, $\mathbf{A} \in \mathbb{R}^{4 \times 4}$ and $\mathbf{B} \in \mathbb{R}^{4 \times 2}$ are as defined in [45, Sec. 6.3.2] (with sampling period $\Delta T = 1$ s), and the driving process \mathbf{w}_n is iid across n , zero-mean, and Gaussian with covariance matrix $\sigma_w^2 \mathbf{I}_2$, where \mathbf{I}_2 denotes the 2×2 identity matrix and σ_w denotes the acceleration noise standard deviation. For the sake of numerical stability, we introduced a small regularization noise to the PMVA state $\mathbf{p}_{k,\text{mva}}$ at each time n , i.e., $\mathbf{p}_{k,\text{mva}} = \mathbf{p}_{k,\text{mva}} + \boldsymbol{\omega}_k$, where $\boldsymbol{\omega}_k$ is iid across k , zero-mean, and Gaussian with covariance matrix $\sigma_a^2 \mathbf{I}_2$ and $\sigma_a = 10^{-3}$ m. We performed 500 simulation runs using 50000 particles, each using the floor plan and agent trajectory shown in Fig. 4. In each simulation run, we generated noisy distance and AOA measurements stacked into the vector $\mathbf{z}_{m,n}^{(j)}$ according to (5) and (6), respectively. For all experiments, the noise standard deviations for the LOS path are $\sigma_{\tau m,n}^{(j)} = 0.05$ m and $\sigma_{\varphi m,n}^{(j)} = 10^\circ$, for single-bounce path are $\sigma_{\tau m,n}^{(j)} = 0.10$ m and $\sigma_{\varphi m,n}^{(j)} = 15^\circ$, and for double-bounce path are $\sigma_{\tau m,n}^{(j)} = 0.15$ m and $\sigma_{\varphi m,n}^{(j)} = 25^\circ$.

⁶Note that the reference method is a combination of [3] and [4] since in [4] statistical model of [3] is extended to AOA measurements of MPCs. However, in contrast to [4], we do not use the component SNRs estimates of MPCs.

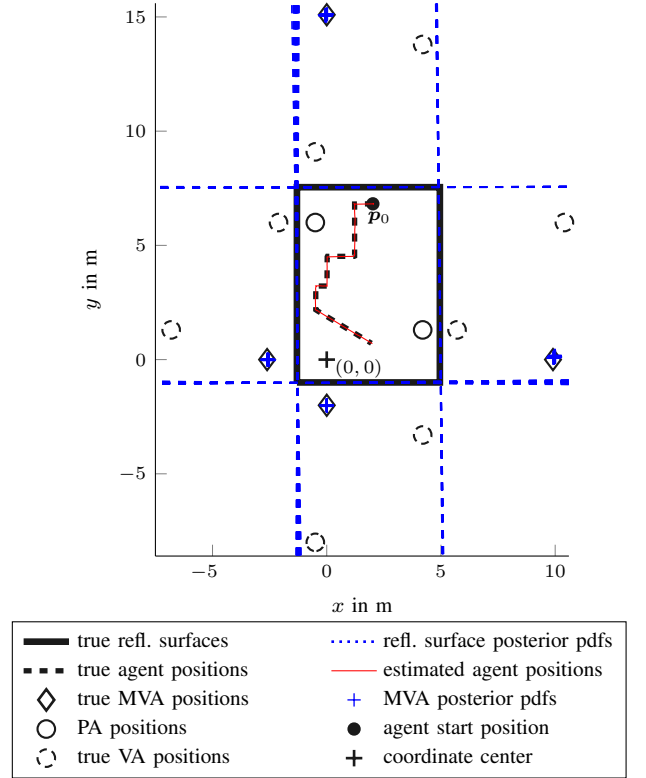


Fig. 4. Considered scenario for performance evaluation in a rectangular room with two PAs, four reflective surfaces and corresponding MVAs and VAs related to the single-bounce paths, as well as agent trajectory.

The detection probability of all paths is $p_{d,ss',n}^{(j)} = p_{d,s,n}^{(j)} = p_d = 0.95$. In addition, a mean number $\mu_{\text{fp}} = 1$ of false positive measurements $\mathbf{z}_{m,n}^{(j)}$ were generated according to the pdf $f_{\text{fp}}(\mathbf{z}_{m,n}^{(j)})$ that is uniform on $[0 \text{ m}, 30 \text{ m}]$. The particles for the initial agent state are drawn from a 4-D uniform distribution with center $\mathbf{x}_0 = [\mathbf{p}_0^T \mathbf{0} \mathbf{0}]^T$, where \mathbf{p}_0 is the starting position of the actual agent trajectory, and the support of each position component about the respective center is given by $[-0.5 \text{ m}, 0.5 \text{ m}]$ and of each velocity component is given by $[-0.1 \text{ m/s}, 0.1 \text{ m/s}]$. At time $n = 0$, the number of MVAs is $S_0 = 0$, i.e., no prior map information is available. The prior distribution for new PMVA states $f_n(\mathbf{y}_{m,n})$ is uniform on the square region given by $[-15 \text{ m}, 15 \text{ m}] \times [-15 \text{ m}, 15 \text{ m}]$ around the center of the floor plan shown in Fig. 4 and the mean number of new PMVA at time n is $\mu_n = 0.05$. The probability of survival is $p_s = 0.999$, the detection threshold is $p_{\text{de}} = 0.5$, and the pruning threshold is $p_{\text{pr}} = 10^{-3}$.

The performance of the different methods discussed is measured in terms of the root mean-square error (RMSE) of the agent position, as well as the optimal subpattern assignment (OSPA) error [46] of VAs and MVAs. The OSPA takes into account data association uncertainty and penalizes an incorrect number of estimated objects. We calculate the optimal subpattern assignment (OSPA) errors based on the Euclidean metric with cutoff parameter $c = 5$ m and order $p = 1$. The mean optimal subpattern assignment (MOSPA) errors, mean RMSEs of each unknown variable are obtained by averaging over all simulation runs.

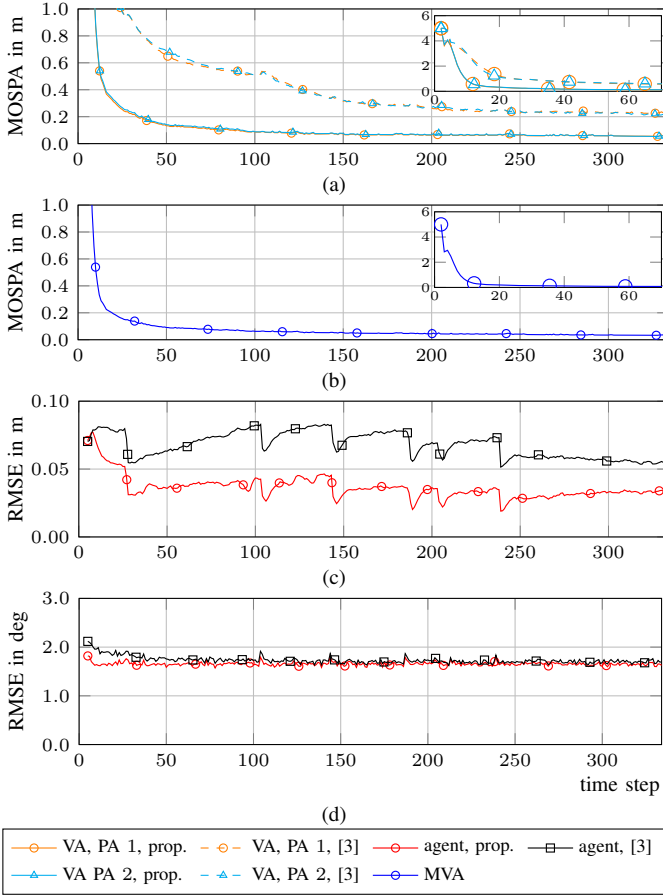


Fig. 5. Performance results for the experiment in Sec. VI-B with constant parameters: (a) MOSPA errors of the VAs of each PA, (b) MOSPA errors of the MVAs, (c) RMSEs of the mobile agent position, (d) RMSEs of the agent orientation.

B. Comparison with Reference Method

In this experiment, we compare the complete version of the proposed MVA-based SLAM algorithm (prop.) and multipath-based SLAM algorithm from [3]. We consider the indoor scenario shown in Figure 4. For ease of comparison, we chose the scenario to be identical to [3]. The scenario consists of four reflective surfaces, i.e., $K = 4$ MVAs, as well as two PAs at positions $\mathbf{p}_{pa}^{(1)} = [-0.5 \ 6]^T$, and $\mathbf{p}_{pa}^{(2)} = [4.2 \ 1.3]^T$. The acceleration noise standard deviation is $\sigma_w = 9 \cdot 10^{-3} \text{ m/s}^2$. Fig. 5a shows the MOSPA error for the two PAs and all associated VAs, Fig. 5b shows the MOSPA error for all MVAs, Fig. 5c shows the RMSE of the mobile agent's position, and Fig. 5d shows the RMSE of the mobile agent's orientation for converged simulation runs, all versus time n . We declare a simulation run to be converged if $\{\forall n : \|\hat{\mathbf{x}}_n - \mathbf{x}_n\| < 0.3\}$. For the proposed algorithm, only one of the 500 simulation runs diverged, but 4 % of the simulation runs diverged for the algorithm in [3]. As an example, Fig. 4 depicts for one simulation run the posterior PDFs represented by particles of the MVA positions and corresponding reflective surfaces as well as estimated agent tracks.

We also present results with varying measurement noise standard deviations. To this end, we introduce factors $f_{\text{std, all}}$ and $f_{\text{std, los}}$. Both factors equally increase all measurement standard deviations $\sigma_{\tau m, n}^{(j)}$ and $\sigma_{\varphi m, n}^{(j)}$ for all $m \in M_n^{(j)} | j \in$

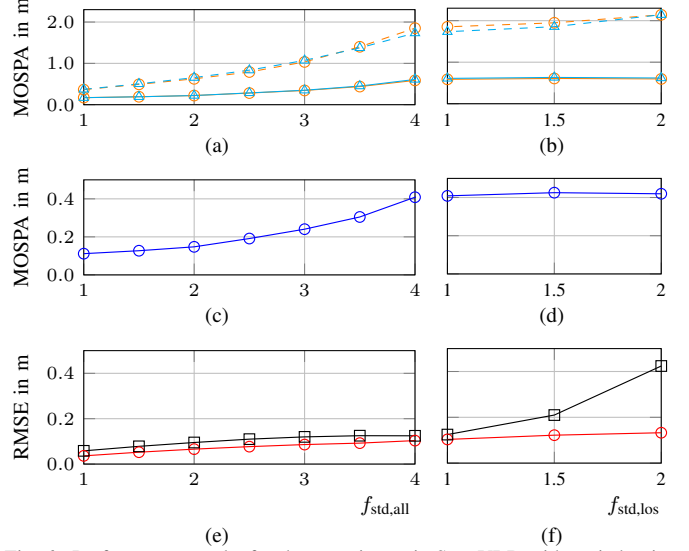


Fig. 6. Performance results for the experiment in Sec. VI-B with varied noise standard deviations: (a) MOSPA errors of the VAs of each PA, (b) MOSPA errors of the MVAs, (c) RMSEs of the mobile agent position, (d) RMSEs of the agent orientation.

$J, n \in \{1, \dots, N\}$ in a multiplicative way concerning their respective base values. While $f_{\text{std, all}}$ affects measurements corresponding to PAs and MVAs, $f_{\text{std, los}}$ affects only those measurement standard deviations corresponding to PAs (i.e., LOS measurements). Fig. 6a to 6f show the mean MOSPA of VAs and PAs, the mean MOSPA of MVAs or the mean agent RMSE, respectively, over all time steps n as a function of $f_{\text{std, all}}$ or $f_{\text{std, los}}$. In particular, in Fig. 6a, 6c and 6e we varied $f_{\text{std, all}}$ and kept $f_{\text{std, los}} \triangleq 1$ fixed, while in Fig. 6b, 6d and 6f we varied $f_{\text{std, los}}$ and kept $f_{\text{std, all}} \triangleq 4$ fixed.

The MOSPA error of the proposed algorithm related to VAs and PAs is shown in Fig. 5a. It can be seen that the MOSPA drops significantly after only a few time steps. In contrast, the algorithm presented in [3] only converges rather slowly to a small mapping error. Furthermore, the MOSPA error of the proposed algorithm converges along the agent track to a smaller value, i.e., to a smaller mapping error. This shows that the proposed MVA-based SLAM algorithm efficiently exploits all measurements for the map features provided by the PAs. Fig. 5b shows the MOSPA error of the MVA positions, which confirms the results seen in Fig. 5a. Finally, the RMSE of the agent position in 5c is slightly increased. At the same time, the map is unstable (i.e., the MOSPA errors are high) but converges to a small value, only increasing slightly during changes of the agent's direction. In contrast, the RMSE of the algorithm from [3] even increases during the straight walk of the agent between $n = 50$ and $n = 100$. Both methods show similar performance in terms of the RMSE of the agent orientation. The VAs MOSPA errors in Figs. 6a to 6d emphasize these observations. Naturally, all error values increase with increasing $f_{\text{std, all}}$. However, the MOSPA errors of the proposed method increase much slower due to the additional information contained in the second-order VAs, which are leveraged by the MVA model. In contrast, the agent RMSE in Fig. 6e remains constant for both methods as there is still enough information available for proper localization,

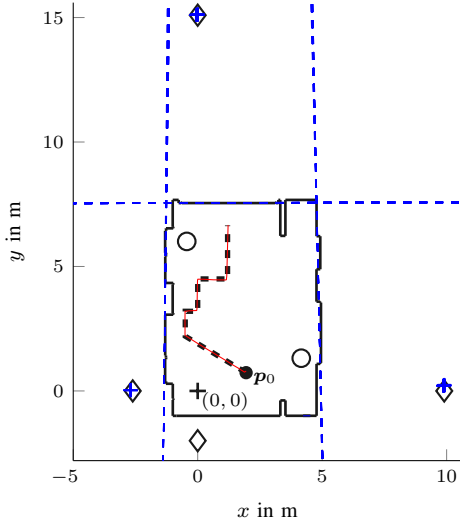


Fig. 7. Considered scenario for performance evaluation in a seminar room with two PAs and four main reflective surfaces and corresponding MVAs, as well as agent trajectory.

which is mainly provided by the PAs. Thus, when additionally increasing $f_{\text{std,los}}$ in Fig. 6f, the RMSE of the algorithm from [3] significantly increases, while the agent RMSE of the proposed algorithm remains approximately constant due to the increased map stability.

C. Validation Using Measured Radio Signals

To validate the applicability of the proposed MVA-based SLAM algorithm to real radio measurements, we use data collected in a seminar room at TU Graz, Austria. More details about the measurement environment and VA calculations can be found in [3], [6], [47]. On the PA side, a dipole-like antenna with an approximately uniform radiation pattern in the azimuth plane and zeros in the floor and ceiling directions was used. At each agent position, the same antenna was deployed multiple times on a 3×3 , 2-D grid to yield a virtual uniform rectangular array with an inter-element spacing of 2 cm. The UWB signals are measured at 220 agent positions along a trajectory with position spacing of 5 cm as shown in Fig. 7 using an M-sequence correlative channel sounder with frequency range 3.1–10.6 GHz. Within the measured band, the actual signal band was selected by a filter with root-raised-cosine impulse response, with a roll-off factor of 0.6, a two-sided 3-dB bandwidth of $B = 1$ GHz and a center frequency of 6 GHz and critically sampled with $T_s = 1/(1.6B)$ and added artificial AWGN such that the output signal-to-noise-ratio is $\text{SNR} = 30$ dB. We apply a variational sparse Bayesian parametric channel estimation algorithm [21] to acquire the $M_n^{(j)}$ distance estimates $z_{dm,n}^{(j)}$ and AOA estimates $z_{\varphi m,n}^{(j)}$ of MPCs. Compared to the synthetic setup, we changed the mean number of false alarm measurements to $\mu_{\text{fp}} = 3$, the detection probability to $p_d = 0.7$, regularization noise standard deviation to $\sigma_a = 2 \cdot 10^{-3}$ m, and the acceleration noise standard deviation to $\sigma_w = 0.0114$ m/s².

Fig. 7 depicts for one simulation run the posterior PDFs represented by particles of the MVA positions and corresponding reflective surfaces as well as estimated agent tracks. The

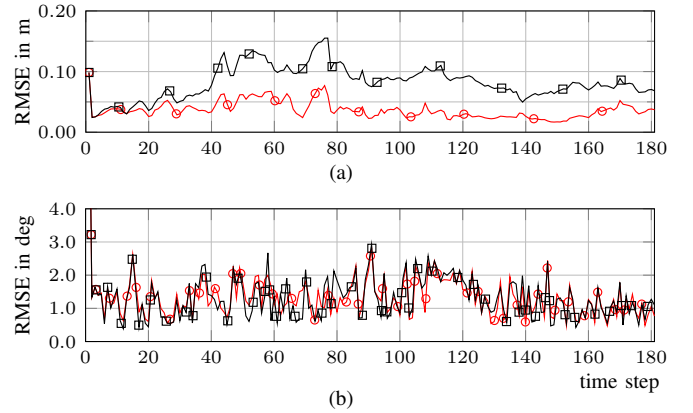


Fig. 8. Performance results for the experiment in VI-C: (a) RMSEs of the mobile agent position and (b) RMSEs of the agent orientation.

proposed algorithm can identify the main reflective surfaces of the room (The lower wall is only visible at the beginning of the agent trace since the reflection coefficient is very low). Although the walls have a rich geometric structure (windows, doors, etc.) and therefore generate many MPCs estimates, i.e. measurements, the proposed algorithm robustly estimates the main walls.

Fig. 8 depicts a comparison of the proposed algorithm and the algorithm in [3] in terms of the agent RMSE. Fig. 8a shows the RMSE of the mobile agent's position, and Fig. 8b shows the RMSE of the mobile agent's orientation for converged simulation runs, all versus time n . The comparison of the position RMSEs shows a similar behavior as for synthetic measurements (see Fig. 5), i.e., the proposed algorithm significantly outperforms the algorithm in [3]. The mapping capability and low agent RMSEs of the proposed algorithm when applied to real radio signals demonstrate the high potential of the proposed algorithm for accurate and robust radio-based localization.

VII. CONCLUSIONS

In this paper, we introduced data fusion for multipath-based SLAM. A key novelty of our approach is to represent each reflective surface in the propagation environment by a single MVA. This representation addresses a key limitation of existing multipath-based SLAM methods which represent every propagation path by a VA and can thus not consistently combine statistical information across multiple paths and base stations. As a result accuracy and mapping speed of existing multipath-based SLAM methods is limited. A key aspect in leveraging the advantages of the introduced MVA-based model, was to check the availability of single-bounce and double-bounce propagation paths at a specific agent position by means of ray-launching. This availability check was directly integrated into the statistical model by providing detection probabilities for probabilistic data association. Our numerical simulation results demonstrated significant improvements in estimation accuracy and mapping speed compared to state-of-the-art multipath-based SLAM methods.

ACKNOWLEDGEMENT

DISTRIBUTION STATEMENT A: Approved for public release. This material is based upon work supported by the

Under Secretary of Defense for Research and Engineering under Air Force Contract No. FA8702-15-D-0001. Any opinions, findings, conclusions, or recommendations expressed in this material are those of the author(s) and do not necessarily reflect the views of the Under Secretary of Defense for Research and Engineering.

REFERENCES

- [1] K. Witrisal, P. Meissner, E. Leitinger, Y. Shen, C. Gustafson, F. Tufvesson, K. Haneda, D. Dardari, A. F. Molisch, A. Conti, and M. Z. Win, "High-accuracy localization for assisted living: 5G systems will turn multipath channels from foe to friend," *IEEE Signal Process. Mag.*, vol. 33, no. 2, pp. 59–70, Mar. 2016.
- [2] C. Gentner, W. Jost, T. Wang, S. Zhang, A. Dammann, and U. C. Fiebig, "Multipath assisted positioning with simultaneous localization and mapping," *IEEE Trans. Wireless Commun.*, vol. 15, no. 9, pp. 6104–6117, Sept. 2016.
- [3] E. Leitinger, F. Meyer, F. Hlawatsch, K. Witrisal, F. Tufvesson, and M. Z. Win, "A belief propagation algorithm for multipath-based SLAM," *IEEE Trans. Wireless Commun.*, vol. 18, no. 12, pp. 5613–5629, Dec. 2019.
- [4] E. Leitinger, S. Grebien, and K. Witrisal, "Multipath-based SLAM exploiting AoA and amplitude information," in *Proc. IEEE ICCW-19*, Shanghai, China, May 2019, pp. 1–7.
- [5] R. Mendrzik, F. Meyer, G. Bauch, and M. Z. Win, "Enabling situational awareness in millimeter wave massive MIMO systems," *IEEE J. Sel. Topics Signal Process.*, vol. 13, no. 5, pp. 1196–1211, Sep. 2019.
- [6] E. Leitinger, P. Meissner, C. Rudisser, G. Dumphart, and K. Witrisal, "Evaluation of position-related information in multipath components for indoor positioning," *IEEE J. Sel. Areas Commun.*, vol. 33, no. 11, pp. 2313–2328, Nov. 2015.
- [7] T. Wilding, S. Grebien, E. Leitinger, U. Mühlmann, and K. Witrisal, "Single-anchor, multipath-assisted indoor positioning with aliased antenna arrays," in *Proc. Asilomar-18*, Pacific Grove, CA, USA, Oct. 2018, pp. 525–531.
- [8] A. Shahmansoori, G. E. Garcia, G. Destino, G. Seco-Granados, and H. Wymeersch, "Position and orientation estimation through millimeter-wave mimo in 5G systems," *IEEE Trans. Wireless Commun.*, vol. 17, no. 3, pp. 1822–1835, Mar. 2018.
- [9] R. Mendrzik, H. Wymeersch, G. Bauch, and Z. Abu-Shaban, "Harnessing NLOS components for position and orientation estimation in 5G millimeter wave MIMO," *IEEE Trans. Wireless Commun.*, vol. 18, no. 1, pp. 93–107, Jan. 2019.
- [10] H. Durrant-Whyte and T. Bailey, "Simultaneous localization and mapping: Part I," *IEEE Robot. Autom. Mag.*, vol. 13, no. 2, pp. 99–110, Jun. 2006.
- [11] M. Dissanayake, P. Newman, S. Clark, H. Durrant-Whyte, and M. Csorba, "A solution to the simultaneous localization and map building (SLAM) problem," *IEEE Trans. Robot. Autom.*, vol. 17, no. 3, pp. 229–241, Jun. 2001.
- [12] M. Montemerlo, S. Thrun, D. Koller, and B. Wegbreit, "FastSLAM: A factored solution to the simultaneous localization and mapping problem," in *Proc. AAAI-02*, Edmonton, Canada, Jul. 2002, pp. 593–598.
- [13] J. Mullane, B.-N. Vo, M. Adams, and B.-T. Vo, "A random-finite-set approach to Bayesian SLAM," *IEEE Trans. Robot.*, vol. 27, no. 2, pp. 268–282, Apr. 2011.
- [14] H. Deusch, S. Reuter, and K. Dietmayer, "The labeled multi-Bernoulli SLAM filter," *IEEE Signal Process. Lett.*, vol. 22, no. 10, pp. 1561–1565, Oct. 2015.
- [15] C. Cadena, L. Carlone, H. Carrillo, Y. Latif, D. Scaramuzza, J. Neira, I. Reid, and J. J. Leonard, "Past, present, and future of simultaneous localization and mapping: Toward the robust-perception age," *IEEE Trans. Robot.*, vol. 32, no. 6, pp. 1309–1332, Dec. 2016.
- [16] X. Chu, Z. Lu, D. Gesbert, L. Wang, X. Wen, M. Wu, and M. Li, "Joint vehicular localization and reflective mapping based on team channel-SLAM," *IEEE Trans. Wireless Commun.*, pp. 1–1, Apr. 2022.
- [17] J. Yang, C.-K. Wen, S. Jin, and X. Li, "Enabling plug-and-play and crowdsourcing SLAM in wireless communication systems," *IEEE Trans. Wireless Commun.*, vol. 21, no. 3, pp. 1453–1468, Aug. 2022.
- [18] A. Richter, "Estimation of Radio Channel Parameters: Models and Algorithms," Ph.D. dissertation, TU Ilmenau, 2005.
- [19] J. Salmi, A. Richter, and V. Koivunen, "Detection and tracking of MIMO propagation path parameters using state-space approach," *IEEE Trans. Signal Process.*, vol. 57, no. 4, pp. 1538–1550, Apr. 2009.
- [20] X. Li, E. Leitinger, A. Venus, and F. Tufvesson, "Sequential detection and estimation of multipath channel parameters using belief propagation," *IEEE Trans. Wireless Commun.*, pp. 1–1, Apr. 2022.
- [21] D. Shutin, W. Wang, and T. Jost, "Incremental sparse Bayesian learning for parameter estimation of superimposed signals," in *Proc. SAMPTA-2013*, no. 1, Sept. 2013, pp. 6–9.
- [22] M. A. Badiu, T. L. Hansen, and B. H. Fleury, "Variational Bayesian inference of line spectra," *IEEE Trans. Signal Process.*, vol. 65, no. 9, pp. 2247–2261, May 2017.
- [23] T. L. Hansen, B. H. Fleury, and B. D. Rao, "Superfast line spectral estimation," *IEEE Trans. Signal Process.*, vol. PP, no. 99, pp. 1–1, Feb. 2018.
- [24] S. Grebien, E. Leitinger, K. Witrisal, and B. H. Fleury, "Super-resolution channel estimation including the dense multipath component — A sparse variational Bayesian approach," 2022, in preparation.
- [25] F. Meyer and J. L. Williams, "Scalable detection and tracking of geometric extended objects," *IEEE Trans. Signal Process.*, vol. 69, pp. 6283–6298, 2021.
- [26] E. Leitinger, P. Meissner, M. Lafer, and K. Witrisal, "Simultaneous localization and mapping using multipath channel information," in *Proc. IEEE ICCW-15*, London, UK, Jun. 2015, pp. 754–760.
- [27] M. Zhu, J. Vieira, Y. Kuang, K. Åström, A. F. Molisch, and F. Tufvesson, "Tracking and positioning using phase information from estimated multipath components," in *Proc. IEEE ICCW-15*, London, UK, Jun. 2015, pp. 712–717.
- [28] H. Kim, K. Granström, L. Gao, G. Battistelli, S. Kim, and H. Wymeersch, "5G mmWave cooperative positioning and mapping using multi-model PHD filter and map fusion," *IEEE Trans. Wireless Commun.*, vol. 19, no. 6, pp. 3782–3795, Mar. 2020.
- [29] H. Kim, K. Granström, L. Svensson, S. Kim, and H. Wymeersch, "PMBM-based SLAM filters in 5G mmWave vehicular networks," *IEEE Trans. Veh. Technol.*, pp. 1–1, May 2022.
- [30] E. Leitinger and F. Meyer, "Data fusion for multipath-based SLAM," in *Proc. Asilomar-20*, Pacific Grove, CA, USA, Oct. 2020, pp. 934–939.
- [31] E. Leitinger, B. Teague, W. Zhang, M. Liang, and F. Meyer, "Data fusion for radio frequency SLAM with robust sampling," in *Proc. Fusion-22*, Linköping, Sweden, Jul. 2022, pp. 1–6.
- [32] J. Borish, "Extension of the image model to arbitrary polyhedra," *JASA*, vol. 75, no. 6, pp. 1827–1836, Mar. 1984.
- [33] J. Kulmer, E. Leitinger, S. Grebien, and K. Witrisal, "Anchorless cooperative tracking using multipath channel information," *IEEE Trans. Wireless Commun.*, vol. 17, no. 4, pp. 2262–2275, Apr. 2018.
- [34] E. Leitinger, A. Venus, B. Teague, and F. Meyer, "Data fusion for multipath-based SLAM: Combining information from multiple propagation paths: Supplementary material," *ArXiv e-prints*, 2022. [Online]. Available: <https://arxiv.org/abs/2211.09241>
- [35] F. Meyer, P. Braca, P. Willett, and F. Hlawatsch, "A scalable algorithm for tracking an unknown number of targets using multiple sensors," *IEEE Trans. Signal Process.*, vol. 65, no. 13, pp. 3478–3493, July 2017.
- [36] F. Meyer, T. Kropfreiter, J. L. Williams, R. Lau, F. Hlawatsch, P. Braca, and M. Z. Win, "Message passing algorithms for scalable multitarget tracking," *Proc. IEEE*, vol. 106, no. 2, pp. 221–259, Feb. 2018.
- [37] M. Bayati, D. Shah, and M. Sharma, "Max-product for maximum weight matching: Convergence, correctness, and LP duality," *IEEE Trans. Inf. Theory*, vol. 54, no. 3, pp. 1241–1251, Mar. 2008.
- [38] M. Chertkov, L. Kroc, F. Krzakala, M. Vergassola, and L. Zdeborová, "Inference in particle tracking experiments by passing messages between images," *PNAS*, vol. 107, no. 17, pp. 7663–7668, Apr. 2010.
- [39] J. Williams and R. Lau, "Approximate evaluation of marginal association probabilities with belief propagation," *IEEE Trans. Aerosp. Electron. Syst.*, vol. 50, no. 4, pp. 2942–2959, Oct. 2014.
- [40] F. Antonio, "Iv.6 - faster line segment intersection," in *Graphics Gems III*. San Francisco: Morgan Kaufmann, 1992, pp. 199–202.
- [41] H. V. Poor, *An Introduction to Signal Detection and Estimation*, 2nd ed. New York: Springer-Verlag, 1994.
- [42] F. Kschischang, B. Frey, and H.-A. Loeliger, "Factor graphs and the sum-product algorithm," *IEEE Trans. Inf. Theory*, vol. 47, no. 2, pp. 498–519, Feb. 2001.
- [43] F. Meyer, O. Hlinka, H. Wymeersch, E. Riegler, and F. Hlawatsch, "Distributed localization and tracking of mobile networks including noncooperative objects," *IEEE Trans. Signal Inf. Process. Netw.*, vol. 2, no. 1, pp. 57–71, Mar. 2016.
- [44] H.-A. Loeliger, "An introduction to factor graphs," *IEEE Signal Process. Mag.*, vol. 21, no. 1, pp. 28–41, Feb. 2004.
- [45] Y. Bar-Shalom, X. R. Li, and T. Kirubarajan, *Estimation with Applications to Tracking and Navigation: Algorithms and Software for Information Extraction*. Hoboken, NJ: John Wiley and Sons, July 2001.
- [46] D. Schuhmacher, B.-T. Vo, and B.-N. Vo, "A consistent metric for performance evaluation of multi-object filters," *IEEE Trans. Signal Process.*, vol. 56, no. 8, pp. 3447–3457, Aug. 2008.
- [47] P. Meissner, E. Leitinger, M. Lafer, and K. Witrisal, "MeasureMINT UWB database," www.spsc.tugraz.at/tools/UWBmeasurements, 2013. [Online]. Available: www.spsc.tugraz.at/tools/UWBmeasurements

Data Fusion for Multipath-Based SLAM: Combining Information from Multiple Propagation Paths: Supplementary Material

Erik Leitinger, Alexander Venus, Bryan Teague, Florian Meyer

June 2022

This manuscript provides additional analysis for the publication “Data Fusion for Multipath-Based SLAM: Combining Information from Multiple Propagation Paths” by the same authors [1].

I. GEOMETRICAL TRANSFORMATIONS

In this section, we derive the non-linear transformations [1, Eq. (3)] and [1, Eq. (4)] in Section [1, Sec. II].

A. Derivation of Transformation from master virtual anchor (MVA) to virtual anchor (VA)

To calculate [1, Eq. (3)], i.e., $\mathbf{p}_{ss,va}^{(j)} = h_{va}(\mathbf{p}_{s,mva}, \mathbf{p}_{pa}^{(j)})$, we define the point $\mathbf{p}_{s,wp}^{(j)}$ given by the intersection of reflective surface s and the line between $\mathbf{p}_{ss,va}^{(j)}$ and $\mathbf{p}_{pa}^{(j)}$. $\mathbf{p}_{s,wp}^{(j)}$ can be expressed as function of $\mathbf{p}_{s,mva} = [p_{1,s,mva} \ p_{2,s,mva}]^T$, i.e.,

$$\mathbf{p}_{s,wp}^{(j)} = \gamma_1 [-p_{2,s,mva} \ p_{1,s,mva}]^T + \frac{\mathbf{p}_{s,mva}}{2} \quad (1)$$

as well as function of $\mathbf{p}_{pa}^{(j)}$ and $\mathbf{p}_{s,mva}$

$$\mathbf{p}_{s,wp}^{(j)} = \gamma_2 \mathbf{p}_{s,mva} + \mathbf{p}_{pa}^{(j)} \quad (2)$$

where the constants γ_1 and γ_2 will be defined in what follows. Furthermore, we express the position of the VA $\mathbf{p}_{ss,va}^{(j)} = [p_{1,ss,va}^{(j)} \ p_{2,ss,va}^{(j)}]^T$ as function of $\mathbf{p}_{pa}^{(j)} = [p_{1,pa}^{(j)} \ p_{2,pa}^{(j)}]^T$ and $\mathbf{p}_{s,mva}$, i.e.,

$$\mathbf{p}_{ss,va}^{(j)} = 2\gamma_2 \mathbf{p}_{s,mva} + \mathbf{p}_{pa}^{(j)}. \quad (3)$$

By combining (1) and (2), we obtain the following expression for γ_1 and γ_2

$$\gamma_1 = \frac{-(1/2 + \gamma_2) p_{2,s,mva} + p_{2,pa}^{(j)}}{p_{1,s,mva}} \quad (4)$$

and

$$\gamma_2 = -\frac{p_{1,pa}^{(j)} p_{1,s,mva} + p_{2,pa}^{(j)} p_{2,s,mva}}{p_{1,s,mva}^2 + p_{2,s,mva}^2} + \frac{1}{2}. \quad (5)$$

By plugging (5) into (3), the nonlinear transformation from MVA to VA is given by

$$\begin{aligned} \mathbf{p}_{ss,va}^{(j)} &= h_{va}(\mathbf{p}_{s,mva}, \mathbf{p}_{pa}^{(j)}) \\ &= -\left(\frac{2p_{1,pa}^{(j)} p_{1,s,mva} + 2p_{2,pa}^{(j)} p_{2,s,mva}}{p_{1,s,mva}^2 + p_{2,s,mva}^2} - 1 \right) \mathbf{p}_{s,mva} + \mathbf{p}_{pa}^{(j)} \\ &= -\left(\frac{2\langle \mathbf{p}_{s,mva}, \mathbf{p}_{pa}^{(j)} \rangle}{\|\mathbf{p}_{s,mva}\|^2} - 1 \right) \mathbf{p}_{s,mva} + \mathbf{p}_{pa}^{(j)} \end{aligned} \quad (6)$$

where $\langle \cdot, \cdot \rangle$ denotes the inner-product between two vectors and $\|\cdot\|$ denotes the Euclidean norm of a vector.

B. Derivation of Transformation from VA to MVA

To calculate [1, Eq. (4)], i.e., $\mathbf{p}_{s,\text{mva}} = h_{\text{mva}}(\mathbf{p}_{ss,\text{va}}, \mathbf{p}_{\text{pa}}^{(j)})$, we define the point $\mathbf{p}_{s,\text{mwp}}$ given by an intersection of reflective surface s and the line between the origin $[00]^T$ and $\mathbf{p}_{s,\text{mva}}$. $\mathbf{p}_{s,\text{mwp}}$ can be expressed as function of $\mathbf{p}_{ss,\text{va}}^{(j)}$, $\mathbf{p}_{\text{pa}}^{(j)}$, and $\mathbf{p}_1^{(j)} = [p_{1,1}^{(j)} \ p_{1,2}^{(j)}]^T = \mathbf{p}_{\text{pa}}^{(j)} - \mathbf{p}_{ss,\text{va}}^{(j)}$, i.e.,

$$\mathbf{p}_{s,\text{mwp}} = \gamma_3 [-p_{2,1} \ p_{1,1}]^T + \frac{\mathbf{p}_{\text{pa}}^{(j)} + \mathbf{p}_{ss,\text{va}}^{(j)}}{2} \quad (7)$$

as well as function of $\mathbf{p}_1^{(j)}$

$$\mathbf{p}_{s,\text{mwp}} = \gamma_4 \mathbf{p}_1^{(j)} \quad (8)$$

where the constants γ_3 and γ_4 will be defined in what follows. Furthermore, we express the position of the VA $\mathbf{p}_{s,\text{mva}}$ as function of $\mathbf{p}_1^{(j)}$, i.e.,

$$\mathbf{p}_{s,\text{mva}} = 2\gamma_4 \mathbf{p}_1^{(j)}. \quad (9)$$

By combining (7) and (8), we obtain the following expression for γ_3 and γ_4

$$\gamma_3 = \frac{\gamma_4 p_{2,1}^{(j)} - 1/2 (p_{2,ss,\text{va}}^{(j)} + p_{2,\text{pa}}^{(j)})}{p_{1,1}^{(j)}} \quad (10)$$

and

$$\gamma_4 = \left(\frac{\langle \mathbf{p}_1^{(j)}, \mathbf{p}_{\text{pa}}^{(j)} \rangle + \langle \mathbf{p}_1^{(j)}, \mathbf{p}_{ss,\text{va}}^{(j)} \rangle}{\|\mathbf{p}_1^{(j)}\|^2} \right). \quad (11)$$

By plugging (11) into (9), the nonlinear transformation from VA to MVA is given by

$$\begin{aligned} \mathbf{p}_{s,\text{mva}} &= h_{\text{mva}}(\mathbf{p}_{s,\text{mva}}, \mathbf{p}_{\text{pa}}^{(j)}) \\ &= \left(\frac{\langle \mathbf{p}_1^{(j)}, \mathbf{p}_{\text{pa}}^{(j)} \rangle + \langle \mathbf{p}_1^{(j)}, \mathbf{p}_{ss,\text{va}}^{(j)} \rangle}{\|\mathbf{p}_1^{(j)}\|^2} \right) \mathbf{p}_1^{(j)} \\ &= \left(\frac{\|\mathbf{p}_{\text{pa}}^{(j)}\|^2 - \|\mathbf{p}_{ss,\text{va}}^{(j)}\|^2}{\|\mathbf{p}_{\text{pa}}^{(j)} - \mathbf{p}_{ss,\text{va}}^{(j)}\|^2} \right) (\mathbf{p}_{\text{pa}}^{(j)} - \mathbf{p}_{ss,\text{va}}^{(j)}). \end{aligned} \quad (12)$$

II. STATISTICAL MODEL

In this section, we derive the expression of $f(\mathbf{y}_{0:n}, \mathbf{x}_{0:n}, \underline{\mathbf{a}}_{1:n}, \bar{\mathbf{a}}_{1:n} | \mathbf{z}_{1:n})$ in [1, Eq. (17)] which is represented by the factor graph in [1, Fig. 3] and provides the basis for the development of a sum-product algorithm (SPA) algorithm for data fusion multipath-based simultaneous localization and mapping (SLAM).

A. Joint Prior PDF

Before presenting derivations, we first define a few sets as follows: $\mathcal{D}_{\underline{\mathbf{a}}_n^{(j)}} \triangleq \{(s, s') \in \tilde{\mathcal{D}}_n^{(j)} : \underline{a}_{ss',n}^{(j)} \neq 0\}$ denotes the set of existing legacy potential MVAs (PMVAs), where $\tilde{\mathcal{D}}_n^{(j)} = (0, 0) \cup \mathcal{D}_n^{(j)}$ with $\mathcal{D}_n^{(j)} \in \{(s, s') \in \mathcal{S}_n \times \mathcal{S}_n\} = \mathcal{D}_{S,n}^{(j)} \cup \mathcal{D}_{D,n}^{(j)}$, which is composed of the index sets for single-bounce propagation path $\mathcal{D}_{S,n}^{(j)}$ and double-bounce propagation paths $\mathcal{D}_{D,n}^{(j)}$, respectively (see [1, Sec. III]). $\mathcal{N}_{\bar{\mathbf{r}}_n^{(j)}} \triangleq \{m \in \{1, \dots, M_n^{(j)}\} : \bar{r}_{m,n}^{(j)} = 1, \bar{a}_{m,n}^{(j)} = 0\}$ denotes the set of existing new PMVAs.

The joint prior probability density function (PDF) of $\mathbf{y}_{0:n} = [\underline{\mathbf{y}}_{0:n}^T, \bar{\mathbf{y}}_{1:n}^T]^T$, $\underline{\mathbf{a}}_{1:n}$, $\bar{\mathbf{a}}_{1:n}$, $\mathbf{x}_{1:n}$, and the number of the measurements $\mathbf{m}_{1:n} \triangleq [\mathbf{M}_1 \cdots \mathbf{M}_n]^T$ factorizes as [2]–[4]

$$\begin{aligned} &f(\mathbf{x}_{0:n}, \mathbf{y}_{0:n}, \underline{\mathbf{a}}_{1:n}, \bar{\mathbf{a}}_{1:n}, \mathbf{m}_{1:n}) \\ &= f(\mathbf{x}_{0:n}, \underline{\mathbf{y}}_{0:n}, \bar{\mathbf{y}}_{1:n}, \underline{\mathbf{a}}_{1:n}, \bar{\mathbf{a}}_{1:n}, \mathbf{m}_{1:n}) \\ &= f(\mathbf{x}_0) \prod_{l=1}^{S_0} f(\mathbf{y}_{l,0}) \prod_{n'=1}^n f(\mathbf{x}_{n'} | \mathbf{x}_{n'-1}) \left(\prod_{s=1}^{S_{n'}-1} f(\underline{\mathbf{y}}_{s,n'} | \mathbf{y}_{s,n'-1}) \right) \end{aligned}$$

$$\times \left(\prod_{j'=2}^J \prod_{s'=1}^{S_{n'}^{(j')}} f^{(j)}(\underline{\mathbf{y}}_{s',n'}^{(j')} | \underline{\mathbf{y}}_{s',n'}^{(j'-1)}) \right) \left(\prod_{j=1}^J f(\bar{\mathbf{p}}_{\text{mva}}^{(j)} | \bar{\mathbf{r}}_{n'}^{(j)}, M_{n'}^{(j)}, \mathbf{x}_{n'}) p(\bar{\mathbf{r}}_{n'}^{(j)}, \underline{\mathbf{a}}_{n'}^{(j)}, \bar{\mathbf{a}}_{n'}^{(j)}, M_{n'}^{(j)} | \underline{\mathbf{y}}_{n'}^{(j)}, \mathbf{x}_{n'}) \right). \quad (13)$$

We determine the prior PDF of new PMVAs $f(\bar{\mathbf{p}}_{\text{mva}}^{(j)} | \bar{\mathbf{r}}_n^{(j)}, M_n^{(j)}, \mathbf{x}_n)$ and the joint conditional prior probability mass function (PMF) $p(\bar{\mathbf{r}}_n^{(j)}, \underline{\mathbf{a}}_n^{(j)}, \bar{\mathbf{a}}_n^{(j)}, M_n^{(j)} | \underline{\mathbf{y}}_n^{(j)}, \mathbf{x}_n)$ in what follows. Before the current measurements are observed, the number of measurements $M_n^{(j)}$ is random. The Poisson PMF of the number of existing new PMVAs evaluated at $|\mathcal{N}_{\bar{\mathbf{r}}_n^{(j)}}|$ is given by

$$p(|\mathcal{N}_{\bar{\mathbf{r}}_n^{(j)}}|) = \mu_n^{|\mathcal{N}_{\bar{\mathbf{r}}_n^{(j)}}|} / |\mathcal{N}_{\bar{\mathbf{r}}_n^{(j)}}|! e^{-\mu_n}. \quad (14)$$

The prior PDF of the new PMVA state $\bar{\mathbf{x}}_n^{(j)}$ conditioned on $\bar{\mathbf{r}}_n^{(j)}$ and $M_n^{(j)}$ is expressed as

$$f(\bar{\mathbf{p}}_{\text{mva}}^{(j)} | \bar{\mathbf{r}}_n^{(j)}, M_n^{(j)}, \mathbf{x}_n) = \prod_{m \in \mathcal{N}_{\bar{\mathbf{r}}_n^{(j)}}} f_n(\bar{\mathbf{p}}_{m,\text{mva}}^{(j)} | \mathbf{x}_n) \prod_{m' \in \{1, \dots, M_n^{(j)}\} \setminus \mathcal{N}_{\bar{\mathbf{r}}_n^{(j)}}} f_d(\bar{\mathbf{p}}_{m',\text{mva}}^{(j)}). \quad (15)$$

The joint conditional prior PMF of the binary existence variables of new PMVAs $\bar{\mathbf{r}}_n \triangleq [\bar{r}_{1,n} \dots \bar{r}_{M_n,n}]$, the association vectors $\underline{\mathbf{a}}_n$ and $\bar{\mathbf{a}}_n$ and the number of the measurements M_n conditioned on \mathbf{x}_n and $\underline{\mathbf{y}}_n^{(j)}$ is obtained as [3]–[5]

$$\begin{aligned} p(\bar{\mathbf{r}}_n^{(j)}, \underline{\mathbf{a}}_n^{(j)}, \bar{\mathbf{a}}_n^{(j)}, M_n^{(j)} | \underline{\mathbf{y}}_n^{(j)}, \mathbf{x}_n) &= \chi_{\bar{\mathbf{r}}_n^{(j)}, \underline{\mathbf{a}}_n^{(j)}, M_n^{(j)}} \left(\prod_{m \in \mathcal{N}_{\bar{\mathbf{r}}_n^{(j)}}} \Gamma_{\underline{\mathbf{a}}_n^{(j)}}(\bar{\mathbf{r}}_{m,n}^{(j)}) \right) \left(\prod_{(s,s') \in \mathcal{D}_{\underline{\mathbf{a}}_n}^{(j)}} p_{\text{dss}'}(\mathbf{p}_n, \underline{\mathbf{y}}_{s,n}^{(j)}, \underline{\mathbf{y}}_{s',n}^{(j)}) \right) \\ &\times \Psi(\underline{\mathbf{a}}_n^{(j)}, \bar{\mathbf{a}}_n^{(j)}) \left(\prod_{(s,s') \in \bar{\mathcal{D}}_n^{(j)} \setminus \mathcal{D}_{\underline{\mathbf{a}}_n^{(j)}}} \left(1 - p_{\text{dss}'}(\mathbf{p}_n, \underline{\mathbf{y}}_{s,n}^{(j)}, \underline{\mathbf{y}}_{s',n}^{(j)}) \right) \right). \end{aligned} \quad (16)$$

where binary indicator function $\Psi(\underline{\mathbf{a}}_n^{(j)}, \bar{\mathbf{a}}_n^{(j)})$ that check consistency for any pair $(\underline{\mathbf{a}}_n^{(j)}, \bar{\mathbf{a}}_n^{(j)})$ of PMVA-oriented and measurement-oriented association variables, read

$$\Psi(\underline{\mathbf{a}}_n^{(j)}, \bar{\mathbf{a}}_n^{(j)}) \triangleq \prod_{(s,s') \in \bar{\mathcal{D}}_n^{(j)}} \prod_{m=1}^{M_n^{(j)}} \Psi(\underline{a}_{ss',n}^{(j)}, \bar{a}_{m,n}^{(j)}) \quad (17)$$

and

$$\Gamma_{\underline{\mathbf{a}}_n^{(j)}}(\bar{\mathbf{r}}_{m,n}^{(j)}) \triangleq \begin{cases} 0, & \bar{r}_{m,n}^{(j)} = 1 \text{ and } a_{ss',n}^{(j)} = m \\ r_{s,n} p_d(\mathbf{p}_n, \underline{\mathbf{p}}_{s,\text{mva}}^{(j)}), & \text{otherwise} \end{cases}. \quad (18)$$

The function

$$p_{\text{dss}'}(\mathbf{p}_n, \underline{\mathbf{y}}_{s,n}^{(j)}, \underline{\mathbf{y}}_{s',n}^{(j)}) \triangleq \begin{cases} r_{s,n} r_{s',n} p_d(\mathbf{p}_n, \underline{\mathbf{p}}_{s,\text{mva}}^{(j)}, \underline{\mathbf{p}}_{s',\text{mva}}^{(j)}), & s \neq s' \wedge (s, s') \neq (0, 0) \\ r_{s,n} p_d(\mathbf{p}_n, \underline{\mathbf{p}}_{s,\text{mva}}^{(j)}), & s = s' \wedge (s, s') \neq (0, 0) \\ p_d(\mathbf{p}_n), & (s, s') = (0, 0) \end{cases} \quad (19)$$

provides the respective detection probability for the line-of-sight (LOS), single-bounce, and double-bounce VAs. The normalization constant $\chi_{\bar{\mathbf{r}}_n^{(j)}, \underline{\mathbf{a}}_n^{(j)}, M_n^{(j)}}$ is given as

$$\chi_{\bar{\mathbf{r}}_n^{(j)}, \underline{\mathbf{a}}_n^{(j)}, M_n^{(j)}} = \left(\frac{\mu_{\text{fp}}^{M_n^{(j)}} e^{-\mu_n - \mu_{\text{fp}}}}{M_n^{(j)}!} \right) \left(\left(\frac{\mu_n}{\mu_{\text{fp}}} \right)^{|\mathcal{N}_{\bar{\mathbf{r}}_n^{(j)}}|} \mu_{\text{fp}}^{-|\mathcal{D}_{\underline{\mathbf{a}}_n^{(j)}}|} \right) \quad (20)$$

where the left-hand-side term (in brackets) is fixed after observing the current measurements given the assumption that the mean number of newly detected PMVAs μ_n and the mean number of false alarms μ_{fp} are known. The right-hand-side term can be merged with factors in the sets $\mathcal{N}_{\bar{\mathbf{r}}_n^{(j)}}$ and $\mathcal{D}_{\underline{\mathbf{a}}_n^{(j)}}$ respectively. The product of the prior PDF of new PMVAs (15) and the joint conditional prior PMF (16) can be written up to the normalization constant as

$$\begin{aligned} &f(\bar{\mathbf{p}}_{\text{mva}}^{(j)} | \bar{\mathbf{r}}_n^{(j)}, M_n^{(j)}, \mathbf{x}_n) p(\bar{\mathbf{r}}_n^{(j)}, \underline{\mathbf{a}}_n^{(j)}, \bar{\mathbf{a}}_n^{(j)}, M_n^{(j)} | \underline{\mathbf{y}}_n^{(j)}, \mathbf{x}_n) \\ &\propto \left(\psi(\underline{\mathbf{a}}_n^{(j)}, \bar{\mathbf{a}}_n^{(j)}) \prod_{(s,s') \in \mathcal{D}_{\underline{\mathbf{a}}_n^{(j)}}} \frac{p_{\text{dss}'}(\mathbf{p}_n, \underline{\mathbf{y}}_{s,n}^{(j)}, \underline{\mathbf{y}}_{s',n}^{(j)})}{\mu_{\text{fp}}} \prod_{(s'',s''') \in \bar{\mathcal{D}}_n^{(j)} \setminus \mathcal{D}_{\underline{\mathbf{a}}_n^{(j)}}} \left(1 - p_{\text{dss}'}(\mathbf{p}_n, \underline{\mathbf{y}}_{s'',n}^{(j)}, \underline{\mathbf{y}}_{s''',n}^{(j)}) \right) \right) \end{aligned}$$

$$\times \left(\prod_{m \in \mathcal{N}_{\bar{\mathbf{r}}_n}^{(j)}} \frac{\mu_n f_n(\bar{\mathbf{p}}_{m',\text{mva}}^{(j)})}{\mu_{\text{fp}}} \Gamma_{\underline{\mathbf{a}}_n}(\bar{\mathbf{r}}_{m,n}^{(j)}) \prod_{m' \in \{1, \dots, M_n^{(j)}\} \setminus \mathcal{N}_{\bar{\mathbf{r}}_n}^{(j)}} f_d(\bar{\mathbf{p}}_{m',\text{mva}}^{(j)}) \right). \quad (21)$$

With some simple manipulations using the definitions of exclusion functions $\Psi(\underline{\mathbf{a}}_n^{(j)}, \bar{\mathbf{a}}_n^{(j)})$ and $\Gamma_{\underline{\mathbf{a}}_n}(\bar{\mathbf{r}}_{m,n}^{(j)})$, Eq. (21) can be rewritten as the product of factors related to the legacy PMVAs and to the new PMVAs respectively, i.e.,

$$\begin{aligned} & f(\bar{\mathbf{p}}_{\text{mva}}^{(j)} | \bar{\mathbf{r}}_n^{(j)}, M_n^{(j)}, \mathbf{x}_n) p(\bar{\mathbf{r}}_n^{(j)}, \underline{\mathbf{a}}_n^{(j)}, \bar{\mathbf{a}}_n^{(j)}, M_n^{(j)} | \underline{\mathbf{y}}_n^{(j)}, \mathbf{x}_n) \\ & \propto \left(\prod_{j=1}^J q_{\text{P1}}(\mathbf{p}_n, \underline{\mathbf{a}}_{00,n}^{(j)}) \prod_{m'=1}^{M_n^{(j)}} \Psi(\underline{\mathbf{a}}_{00,n'}^{(j)}, \bar{\mathbf{a}}_{m',n'}^{(j)}) \right) \left(\prod_{s=1}^{S_n^{(j)}} q_{\text{S1}}(\underline{\mathbf{y}}_{s,n}^{(j)}, \underline{\mathbf{a}}_{ss,n}^{(j)}, \mathbf{p}_n) \left(\prod_{m'=1}^{M_n^{(j)}} \Psi(\underline{\mathbf{a}}_{ss,n}^{(j)}, \bar{\mathbf{a}}_{m',n}^{(j)}) \right) \right) \\ & \times \prod_{s'=1, s' \neq s}^{S_n^{(j)}} q_{\text{D1}}(\underline{\mathbf{y}}_{s,n}^{(j)}, \underline{\mathbf{y}}_{s',n}^{(j)}, \underline{\mathbf{a}}_{ss',n}^{(j)}, \mathbf{p}_n) \prod_{m'=1}^{M_n^{(j)}} \Psi(\underline{\mathbf{a}}_{ss',n}^{(j)}, \bar{\mathbf{a}}_{m',n}^{(j)}) \left(\prod_{m=1}^{M_n^{(j)}} \bar{q}_{\text{S1}}(\bar{\mathbf{y}}_{m,n}^{(j)}, \bar{\mathbf{a}}_{m,n}^{(j)}, \mathbf{p}_n) \right). \quad (22) \end{aligned}$$

We note that the factor $\prod_{m'=1}^{M_n^{(j)}} \Psi(\underline{\mathbf{a}}_{00,n'}^{(j)}, \bar{\mathbf{a}}_{m',n'}^{(j)})$ in (13) considers the joint data association with respect to the LOS component [3] that is assumed to always exist (but may not always be detected). The functions related to the physical anchor (PA) $q_{\text{P1}}(\mathbf{p}_n, \underline{\mathbf{a}}_{00,n}^{(j)})$ and to the legacy PMVA states $q_{\text{S1}}(\underline{\mathbf{y}}_{s,n}^{(j)}, \underline{\mathbf{a}}_{ss,n}^{(j)}, \mathbf{p}_n) = q_{\text{S1}}(\underline{\mathbf{r}}_{s,n}^{(j)}, \underline{\mathbf{p}}_{s,\text{mva}}^{(j)}, \underline{\mathbf{a}}_{ss,n}^{(j)}, \mathbf{p}_n)$ and $q_{\text{D1}}(\underline{\mathbf{y}}_{s,n}^{(j)}, \underline{\mathbf{y}}_{s',n}^{(j)}, \underline{\mathbf{a}}_{ss',n}^{(j)}, \mathbf{p}_n) = q_{\text{D1}}(\underline{\mathbf{p}}_{s,\text{mva}}^{(j)}, \underline{\mathbf{r}}_{s,n}^{(j)}, \underline{\mathbf{p}}_{s',\text{mva}}^{(j)}, \underline{\mathbf{r}}_{s',n}^{(j)}, \underline{\mathbf{a}}_{ss',n}^{(j)}, \mathbf{p}_n)$ are respectively given by

$$q_{\text{P1}}(\mathbf{p}_n, \underline{\mathbf{a}}_{00,n}^{(j)}) \triangleq \begin{cases} \frac{p_d(\mathbf{p}_n)}{\mu_{\text{fp}}}, & \underline{\mathbf{a}}_{00,n}^{(j)} \in \mathcal{M}_n^{(j)} \\ 1 - p_d(\mathbf{p}_n), & \underline{\mathbf{a}}_{00,n}^{(j)} = 0 \end{cases}, \quad (23)$$

$$q_{\text{S1}}(\underline{\mathbf{p}}_{s,\text{mva}}^{(j)}, \underline{\mathbf{r}}_{s,n}^{(j)} = 1, \underline{\mathbf{a}}_{ss,n}^{(j)}, \mathbf{p}_n) \triangleq \begin{cases} \frac{p_d(\mathbf{p}_n, \underline{\mathbf{p}}_{s,\text{mva}}^{(j)})}{\mu_{\text{fp}}}, & \underline{\mathbf{a}}_{ss,n}^{(j)} \in \mathcal{M}_n^{(j)} \\ 1 - p_d(\mathbf{p}_n, \underline{\mathbf{p}}_{s,\text{mva}}^{(j)}), & \underline{\mathbf{a}}_{ss,n}^{(j)} = 0 \end{cases}, \quad (24)$$

$$q_{\text{S1}}(\underline{\mathbf{p}}_{s,\text{mva}}^{(j)}, \underline{\mathbf{r}}_{s,n}^{(j)} = 0, \underline{\mathbf{a}}_{ss,n}^{(j)}, \mathbf{p}_n) \triangleq \delta(\underline{\mathbf{a}}_{ss,n}^{(j)}),$$

$$q_{\text{D1}}(\underline{\mathbf{p}}_{s,\text{mva}}^{(j)}, \underline{\mathbf{r}}_{s,n}^{(j)} = 1, \underline{\mathbf{p}}_{s',\text{mva}}^{(j)}, \underline{\mathbf{r}}_{s',n}^{(j)} = 1, \underline{\mathbf{a}}_{ss',n}^{(j)}, \mathbf{p}_n) \triangleq \begin{cases} \frac{p_d(\mathbf{p}_n, \underline{\mathbf{p}}_{s,\text{mva}}^{(j)}, \underline{\mathbf{p}}_{s',\text{mva}}^{(j)})}{\mu_{\text{fp}}}, & \underline{\mathbf{a}}_{ss',n}^{(j)} \in \mathcal{M}_n^{(j)} \\ 1 - p_d(\mathbf{p}_n, \underline{\mathbf{p}}_{s,\text{mva}}^{(j)}, \underline{\mathbf{p}}_{s',\text{mva}}^{(j)}), & \underline{\mathbf{a}}_{ss',n}^{(j)} = 0 \end{cases}, \quad (25)$$

and $q_{\text{D1}}(\underline{\mathbf{p}}_{s,\text{mva}}^{(j)}, \underline{\mathbf{r}}_{s,n}^{(j)}, \underline{\mathbf{p}}_{s',\text{mva}}^{(j)}, \underline{\mathbf{r}}_{s',n}^{(j)}, \underline{\mathbf{a}}_{ss',n}^{(j)}, \mathbf{p}_n) \triangleq \delta(\underline{\mathbf{a}}_{ss',n}^{(j)})$ if $\underline{\mathbf{r}}_{s,n}^{(j)} = 0$ or $\underline{\mathbf{r}}_{s',n}^{(j)} = 0$. The function $\bar{q}_{\text{S1}}(\bar{\mathbf{y}}_{m,\text{mva}}^{(j)}, \bar{\mathbf{a}}_{m,n}^{(j)}, \mathbf{p}_n) = \bar{q}_{\text{S1}}(\bar{\mathbf{p}}_{m,\text{mva}}^{(j)}, \bar{\mathbf{r}}_{s,n}^{(j)}, \bar{\mathbf{a}}_{m,n}^{(j)}, \mathbf{p}_n)$ related to new PMVA states reads

$$\bar{q}_{\text{S1}}(\bar{\mathbf{p}}_{m,\text{mva}}^{(j)}, \bar{\mathbf{r}}_{s,n}^{(j)} = 1, \bar{\mathbf{a}}_{m,n}^{(j)}, \mathbf{p}_n) \triangleq \begin{cases} 0, & \bar{\mathbf{a}}_{m,n}^{(j)} \in \tilde{\mathcal{D}}_n^{(j)} \\ \frac{\mu_n f_n(\bar{\mathbf{p}}_{m,\text{mva}}^{(j)} | \mathbf{p}_n)}{\mu_{\text{fp}}}, & \bar{\mathbf{a}}_{m,n}^{(j)} = 0 \end{cases} \quad (26)$$

$$\text{and } \bar{q}_{\text{S1}}(\bar{\mathbf{p}}_{m,\text{mva}}^{(j)}, \bar{\mathbf{r}}_{s,n}^{(j)} = 0, \bar{\mathbf{a}}_{m,n}^{(j)}, \mathbf{p}_n) \triangleq 1.$$

Finally, by inserting (22) into (13), the joint prior PDF can be rewritten as

$$\begin{aligned} & f(\mathbf{x}_{0:n}, \mathbf{y}_{0:n}, \underline{\mathbf{a}}_{1:n}, \bar{\mathbf{a}}_{1:n}, \mathbf{m}_{1:n}) \\ & \propto \left(f(\mathbf{x}_0) \prod_{l=1}^{S_0} f(\mathbf{y}_{l,0}) \right) \prod_{n'=1}^n f(\mathbf{x}_{n'} | \mathbf{x}_{n'-1}) \left(\prod_{j=1}^J q_{\text{P1}}(\mathbf{p}_{n'}, \underline{\mathbf{a}}_{00,n'}^{(j)}) \prod_{m'=1}^{M_{n'}^{(j)}} \Psi(\underline{\mathbf{a}}_{00,n'}^{(j)}, \bar{\mathbf{a}}_{m',n'}^{(j)}) \right) \left(\prod_{s'=1}^{S_{n'-1}} f(\underline{\mathbf{y}}_{s',n'} | \underline{\mathbf{y}}_{s',n'-1}) \right) \\ & \times \left(\prod_{j'=2}^J \left(\prod_{s'=1}^{S_{n'}^{(j')}} f(\underline{\mathbf{y}}_{s',n'}^{(j')} | \underline{\mathbf{y}}_{s',n'}^{(j'-1)}) \right) \right) \prod_{j=1}^J \left(\prod_{s=1}^{S_{n'}^{(j)}} q_{\text{S1}}(\underline{\mathbf{y}}_{s,n'}^{(j)}, \underline{\mathbf{a}}_{ss,n'}^{(j)}, \mathbf{p}_{n'}) \left(\prod_{m'=1}^{M_{n'}^{(j)}} \Psi(\underline{\mathbf{a}}_{ss,n'}^{(j)}, \bar{\mathbf{a}}_{m',n'}^{(j)}) \right) \right) \end{aligned}$$

$$\times \prod_{s'=1, s' \neq s}^{S_{n'}^{(j)}} q_{\text{D1}}(\underline{\mathbf{y}}_{s,n'}, \underline{\mathbf{y}}_{s',n'}, \underline{\mathbf{a}}_{ss',n'}, \mathbf{p}_{n'}) \prod_{m'=1}^{M_{n'}^{(j)}} \Psi(\underline{\mathbf{a}}_{ss',n'}, \bar{\mathbf{a}}_{m',n'}^{(j)}) \left(\prod_{m=1}^{M_{n'}^{(j)}} \bar{q}_{\text{S1}}(\bar{\mathbf{y}}_{m,n'}, \bar{\mathbf{a}}_{m,n'}^{(j)}, \mathbf{p}_{n'}) \right) \quad (27)$$

B. Joint Likelihood Function

Assume that the measurements \mathbf{z}_n are independent across n , the conditional PDF of $\mathbf{z}_{1:n}$ given $\mathbf{x}_{1:n}$, $\underline{\mathbf{y}}_{1:n}$, $\bar{\mathbf{y}}_{1:n}$, $\underline{\mathbf{a}}_{1:n}$, $\bar{\mathbf{a}}_{1:n}$, and the number of measurements $\mathbf{m}_{1:n}$ is given by

$$f(\mathbf{z}_{1:n} | \mathbf{x}_{1:n}, \underline{\mathbf{y}}_{1:n}, \bar{\mathbf{y}}_{1:n}, \underline{\mathbf{a}}_{1:n}, \bar{\mathbf{a}}_{1:n}, \mathbf{m}_{1:n}) = \prod_{n'=1}^n f(\mathbf{z}_{n'} | \mathbf{x}_{n'}, \underline{\mathbf{y}}_{n'}, \bar{\mathbf{y}}_{n'}, \underline{\mathbf{a}}_{n'}, \bar{\mathbf{a}}_{n'}, M_{n'}) \quad (28)$$

for \mathbf{z}_n and $f(\mathbf{z}_n | \mathbf{x}_n, \underline{\mathbf{y}}_n, \bar{\mathbf{y}}_n, \underline{\mathbf{a}}_n, \bar{\mathbf{a}}_n, M_n) = 0$ otherwise. Assuming that the measurements $\mathbf{z}_{m,n}$ are conditionally independent across m given $\underline{\mathbf{y}}_{k,n}$, $\bar{\mathbf{y}}_{m,n}$, $\underline{\mathbf{a}}_{k,n}$, $\bar{\mathbf{a}}_{m,n}$, and M_n [3], [6], Eq. (28) factorizes as

$$\begin{aligned} f(\mathbf{z}_{1:n} | \mathbf{x}_{1:n}, \underline{\mathbf{y}}_{1:n}, \bar{\mathbf{y}}_{1:n}, \underline{\mathbf{a}}_{1:n}, \bar{\mathbf{a}}_{1:n}, \mathbf{m}_{1:n}) \\ = \prod_{n'=1}^n C(\mathbf{z}_{n'}) \left(\prod_{(s,s') \in \mathcal{D}_{\underline{\mathbf{a}}_n^{(j)}, \underline{\mathbf{r}}_{ss',n}^{(j)}}} \frac{f_{ss'}(\mathbf{z}_{\underline{\mathbf{a}}_{ss',n'}, n'} | \mathbf{p}_n, \underline{\mathbf{p}}_{s,\text{mva}}^{(j)}, \underline{\mathbf{p}}_{s',\text{mva}}^{(j)})}{f_{\text{fp}}(\underline{\mathbf{a}}_{ss',n'}^{(j)})} \right) \left(\prod_{m \in \mathcal{N}_{\bar{\mathbf{r}}_n^{(j)}}} \frac{f(\mathbf{z}_{m,n} | \mathbf{p}_n, \bar{\mathbf{p}}_{m,\text{mva}}^{(j)})}{f_{\text{fp}}(\mathbf{z}_{m,n'})} \right) \end{aligned} \quad (29)$$

where $\mathcal{D}_{\underline{\mathbf{a}}_n^{(j)}, \underline{\mathbf{r}}_{ss',n}^{(j)}} \triangleq \{(s, s') \in \mathcal{D}_{\underline{\mathbf{a}}_n^{(j)}} : \underline{\mathbf{r}}_{s,n}^{(j)} \neq 0 \wedge \underline{\mathbf{r}}_{s',n}^{(j)} \neq 0\}$ considers non existent PMVAs and

$$f_{ss'}(\mathbf{z}_{m,n} | \mathbf{p}_n, \underline{\mathbf{p}}_{s,\text{mva}}^{(j)}, \underline{\mathbf{p}}_{s',\text{mva}}^{(j)}) \triangleq \begin{cases} f(\mathbf{z}_{m,n} | \mathbf{p}_n, \underline{\mathbf{p}}_{s,\text{mva}}^{(j)}, \underline{\mathbf{p}}_{s',\text{mva}}^{(j)}), & s \neq s' \wedge (s, s') \neq (0, 0) \\ f(\mathbf{z}_{m,n} | \mathbf{p}_n, \underline{\mathbf{p}}_{s,\text{mva}}^{(j)}), & s = s' \wedge (s, s') \neq (0, 0) \\ f(\mathbf{z}_{m,n} | \mathbf{p}_n), & (s, s') = (0, 0) \end{cases} \quad (30)$$

provides the respective likelihood function for LOS, single-bounce and double-bounce VAs. Since the normalization factor $C(\mathbf{z}_n) = \prod_{m=1}^{M_n} f_{\text{fa}}(\mathbf{z}_{m,n})$ depending on \mathbf{z}_n and M_n is fixed after the current measurement \mathbf{z}_n is observed and using $\mathbf{y}_{1:n} = [\underline{\mathbf{y}}_{1:n}^T, \bar{\mathbf{y}}_{1:n}^T]^T$, the likelihood function in (29) can be rewritten up to the normalization constant as

$$\begin{aligned} f(\mathbf{z}_{1:n} | \mathbf{x}_{1:n}, \underline{\mathbf{y}}_{1:n}, \bar{\mathbf{y}}_{1:n}, \underline{\mathbf{a}}_{1:n}, \bar{\mathbf{a}}_{1:n}, \mathbf{m}_{1:n}) \\ \propto \prod_{n'=1}^n \prod_{j=1}^J \left(q_{\text{P2}}(\mathbf{x}_{n'}, \underline{\mathbf{a}}_{00,n'}^{(j)}; \mathbf{z}_{n'}^{(j)}) \prod_{s=1}^{S_{n'}^{(j)}} q_{\text{S2}}(\underline{\mathbf{y}}_{s,n'}, \underline{\mathbf{a}}_{ss,n'}^{(j)}, \mathbf{x}_{n'}; \mathbf{z}_{n'}^{(j)}) \prod_{s'=1, s' \neq s}^{S_{n'}^{(j)}} q_{\text{D2}}(\underline{\mathbf{y}}_{s,n'}, \underline{\mathbf{y}}_{s',n'}^{(j)}, \underline{\mathbf{a}}_{ss',n'}^{(j)}, \mathbf{x}_{n'}; \mathbf{z}_{n'}^{(j)}) \right) \\ \times \prod_{m=1}^{M_{n'}^{(j)}} \bar{q}_{\text{S2}}(\bar{\mathbf{y}}_{m,n'}, \bar{\mathbf{a}}_{m,n'}^{(j)}, \mathbf{x}_{n'}; \mathbf{z}_{n'}^{(j)}) \end{aligned} \quad (31)$$

where the factors related to the PA $q_{\text{P2}}(\mathbf{x}_n, \underline{\mathbf{a}}_{00,n}^{(j)}; \mathbf{z}_n^{(j)})$ is given by

$$q_{\text{P2}}(\mathbf{x}_n, \underline{\mathbf{a}}_{00,n}^{(j)}; \mathbf{z}_n^{(j)}) \triangleq \begin{cases} \frac{f(\mathbf{z}_{m,n}^{(j)} | \mathbf{p}_n)}{f_{\text{fp}}(\mathbf{z}_{m,n}^{(j)})}, & \underline{\mathbf{a}}_{00,n}^{(j)} = m \in \mathcal{M}_n^{(j)} \\ 1, & \underline{\mathbf{a}}_{00,n}^{(j)} = 0 \end{cases} \quad (32)$$

and the factors related to legacy PMVA states $q_{\text{S2}}(\underline{\mathbf{y}}_{s,n}^{(j)}, \underline{\mathbf{a}}_{ss,n}^{(j)}, \mathbf{x}_n; \mathbf{z}_n^{(j)}) = q_{\text{S2}}(\underline{\mathbf{r}}_{s,n}^{(j)}, \underline{\mathbf{p}}_{s,\text{mva}}^{(j)}, \underline{\mathbf{a}}_{ss,n}^{(j)}, \mathbf{x}_n; \mathbf{z}_n^{(j)})$ and $q_{\text{D2}}(\underline{\mathbf{y}}_{s,n}^{(j)}, \underline{\mathbf{y}}_{s',n}^{(j)}, \underline{\mathbf{a}}_{ss',n}^{(j)}, \mathbf{x}_n; \mathbf{z}_n^{(j)}) = q_{\text{D2}}(\underline{\mathbf{p}}_{s,\text{mva}}^{(j)}, \underline{\mathbf{r}}_{s,n}^{(j)}, \underline{\mathbf{p}}_{s',\text{mva}}^{(j)}, \underline{\mathbf{r}}_{s',n}^{(j)}, \underline{\mathbf{a}}_{ss',n}^{(j)}, \mathbf{x}_n; \mathbf{z}_n^{(j)})$ are given respectively by

$$q_{\text{S2}}(\underline{\mathbf{p}}_{s,\text{mva}}^{(j)}, \underline{\mathbf{r}}_{s,n}^{(j)} = 1, \underline{\mathbf{a}}_{ss,n}^{(j)}, \mathbf{x}_n; \mathbf{z}_n^{(j)}) \triangleq \begin{cases} \frac{f(\mathbf{z}_{m,n}^{(j)} | \mathbf{p}_n, \underline{\mathbf{p}}_{s,\text{mva}}^{(j)})}{f_{\text{fp}}(\mathbf{z}_{m,n}^{(j)})}, & \underline{\mathbf{a}}_{ss,n}^{(j)} = m \in \mathcal{M}_n^{(j)} \\ 1, & \underline{\mathbf{a}}_{ss,n}^{(j)} = 0 \end{cases} \quad (33)$$

and $q_{\text{S2}}(\mathbf{p}_{s,\text{mva}}^{(j)}, r_{s,n}^{(j)} = 0, \underline{a}_{ss,n}^{(j)}, \mathbf{x}_n; \mathbf{z}_n^{(j)}) \triangleq 1$ and by

$$q_{\text{D2}}(\mathbf{p}_{s,\text{mva}}^{(j)}, r_{s,n}^{(j)} = 1, \mathbf{p}_{s',\text{mva}}^{(j)}, r_{s',n}^{(j)} = 1, \underline{a}_{ss',n}^{(j)}, \mathbf{x}_n; \mathbf{z}_n^{(j)}) \triangleq \begin{cases} \frac{f(\mathbf{z}_{m,n}^{(j)} | \mathbf{p}_n, \mathbf{p}_{s,\text{mva}}^{(j)}, \mathbf{p}_{s',\text{mva}}^{(j)})}{f_{\text{fp}}(\mathbf{z}_{m,n}^{(j)})}, & a_{ss'}^{(j)} = m \in \mathcal{M}_n^{(j)} \\ 1, & a_{ss'}^{(j)} = 0 \end{cases} \quad (34)$$

and $q_{\text{D2}}(\mathbf{p}_{s,\text{mva}}^{(j)}, r_{s,n}^{(j)}, \mathbf{p}_{s',\text{mva}}^{(j)}, r_{s',n}^{(j)}, \underline{a}_{ss',n}^{(j)}, \mathbf{x}_n; \mathbf{z}_n^{(j)}) \triangleq 1$ if $r_{s,n}^{(j)} = 0$ or $r_{s',n}^{(j)} = 0$. The factor related to new PMVA states $\bar{q}_{\text{S2}}(\bar{\mathbf{y}}_{m,\text{mva}}^{(j)}, \bar{a}_{m,n}^{(j)}, \mathbf{x}_n; \mathbf{z}_n^{(j)}) = \bar{q}_{\text{S2}}(\bar{\mathbf{p}}_{m,\text{mva}}^{(j)}, \bar{r}_{s,n}^{(j)}, \bar{a}_{m,n}^{(j)}, \mathbf{x}_n; \mathbf{z}_n^{(j)})$ is given by

$$\bar{q}_{\text{S2}}(\bar{\mathbf{p}}_{m,\text{mva}}^{(j)}, \bar{r}_{s,n}^{(j)} = 1, \bar{a}_{m,n}^{(j)}, \mathbf{x}_n; \mathbf{z}_n^{(j)}) \triangleq \begin{cases} 0, & \bar{a}_{m,n}^{(j)} \in \tilde{\mathcal{D}}_n^{(j)} \\ \frac{f(\mathbf{z}_{m,n}^{(j)} | \mathbf{p}_n, \mathbf{p}_{m,\text{mva}}^{(j)})}{f_{\text{fp}}(\mathbf{z}_{m,n}^{(j)})}, & \bar{a}_{m,n}^{(j)} = 0 \end{cases} \quad (35)$$

and $\bar{q}_{\text{S2}}(\bar{\mathbf{p}}_{m,\text{mva}}^{(j)}, \bar{r}_{s,n}^{(j)} = 0, \bar{a}_{m,n}^{(j)}, \mathbf{x}_n; \mathbf{z}_n^{(j)}) \triangleq 1$.

C. Joint Posterior PDF

We derive the factorization of $f(\mathbf{y}_{0:n}, \mathbf{x}_{0:n}, \underline{\mathbf{a}}_{1:n}, \bar{\mathbf{a}}_{1:n} | \mathbf{z}_{1:n})$ considering that the measurements $\mathbf{z}_{1:n}$ are observed and thus fixed (consequently M_n is fixed as well). By using Bayes'rule and by exploiting the fact that \mathbf{z}_n implies M_n according to (29), we obtain [5], [7]

$$\begin{aligned} f(\mathbf{y}_{0:n}, \mathbf{x}_{0:n}, \underline{\mathbf{a}}_{1:n}, \bar{\mathbf{a}}_{1:n} | \mathbf{z}_{1:n}) &= \sum_{M'_1=0}^{\infty} \sum_{M'_2=0}^{\infty} \cdots \sum_{M'_n=0}^{\infty} f(\mathbf{y}_{0:n}, \mathbf{x}_{0:n}, \underline{\mathbf{a}}_{1:n}, \bar{\mathbf{a}}_{1:n}, \mathbf{m}'_{1:n} | \mathbf{z}_{1:n}) \\ &= \sum_{M'_1=0}^{\infty} \sum_{M'_2=0}^{\infty} \cdots \sum_{M'_n=0}^{\infty} f(\mathbf{z}_{1:n} | \mathbf{x}_{1:n}, \mathbf{y}_{1:n}, \underline{\mathbf{a}}_{1:n}, \bar{\mathbf{a}}_{1:n}, \mathbf{m}'_{1:n}) f(\mathbf{y}_{0:n}, \mathbf{x}_{0:n}, \underline{\mathbf{a}}_{1:n}, \bar{\mathbf{a}}_{1:n}, \mathbf{m}'_{1:n}) \end{aligned} \quad (36)$$

Using the factorized joint prior PDF (27) and the factorized joint likelihood function (31) the joint posterior PDF (36) can be rearranged as

$$\begin{aligned} &f(\mathbf{y}_{0:n}, \mathbf{x}_{0:n}, \underline{\mathbf{a}}_{1:n}, \bar{\mathbf{a}}_{1:n} | \mathbf{z}_{1:n}) \\ &\propto \left(f(\mathbf{x}_0) \prod_{l=1}^{S_0} f(\mathbf{y}_{l,0}) \right) \prod_{n'=1}^n f(\mathbf{x}_{n'} | \mathbf{x}_{n'-1}) \left(\prod_{j=1}^J q_{\text{P1}}(\mathbf{p}_{n'}, \underline{a}_{00,n'}^{(j)}) q_{\text{P2}}(\mathbf{x}_{n'}, \underline{a}_{00,n'}^{(j)}; \mathbf{z}_{n'}^{(j)}) \prod_{m'=1}^{M_{n'}^{(j)}} \Psi(\underline{a}_{00,n'}^{(j)}, \bar{a}_{m',n'}^{(j)}) \right) \\ &\times \left(\prod_{s'=1}^{S_{n'-1}} f(\mathbf{y}_{s',n'} | \mathbf{y}_{s',n'-1}) \right) \left(\prod_{j'=2}^J \left(\prod_{s'=1}^{S_{n'}^{(j')}} f^{(j)}(\mathbf{y}_{s',n'}^{(j')} | \mathbf{y}_{s',n'}^{(j'-1)}) \right) \right) \prod_{j=1}^J \left(\prod_{s=1}^{S_{n'}^{(j)}} q_{\text{S1}}(\mathbf{y}_{s,n'}^{(j)}, \underline{a}_{ss,n'}^{(j)}, \mathbf{p}_{n'}) q_{\text{S2}}(\mathbf{y}_{s,n'}^{(j)}, \underline{a}_{ss,n'}^{(j)}, \mathbf{x}_{n'}; \mathbf{z}_{n'}^{(j)}) \right) \\ &\times \left(\prod_{m'=1}^{M_{n'}^{(j)}} \Psi(\underline{a}_{ss,n'}^{(j)}, \bar{a}_{m',n'}^{(j)}) \right) \prod_{s'=1, s' \neq s}^{S_{n'}^{(j)}} q_{\text{D1}}(\mathbf{y}_{s,n'}^{(j)}, \mathbf{y}_{s',n'}^{(j)}, \underline{a}_{ss',n'}^{(j)}, \mathbf{p}_{n'}) q_{\text{D2}}(\mathbf{y}_{s,n'}^{(j)}, \mathbf{y}_{s',n'}^{(j)}, \underline{a}_{ss',n'}^{(j)}, \mathbf{x}_{n'}; \mathbf{z}_{n'}^{(j)}) \prod_{m'=1}^{M_{n'}^{(j)}} \Psi(\underline{a}_{ss',n'}^{(j)}, \bar{a}_{m',n'}^{(j)}) \\ &\times \left(\prod_{m=1}^{M_{n'}^{(j)}} \bar{q}_{\text{S1}}(\bar{\mathbf{y}}_{m,n'}, \bar{a}_{m,n'}^{(j)}, \mathbf{p}_{n'}) \bar{q}_{\text{S2}}(\bar{\mathbf{y}}_{m,n'}, \bar{a}_{m,n'}^{(j)}, \mathbf{x}_{n'}; \mathbf{z}_{n'}^{(j)}) \right) \end{aligned} \quad (37)$$

The factors related to the legacy PMVAs and to the new PMVAs can be simplified as $q_{\text{P}}(\mathbf{x}_{n'}, \underline{a}_{00,n'}^{(j)}; \mathbf{z}_{n'}^{(j)}) \triangleq q_{\text{P1}}(\mathbf{p}_{n'}, \underline{a}_{00,n'}^{(j)}) q_{\text{P2}}(\mathbf{x}_{n'}, \underline{a}_{00,n'}^{(j)}; \mathbf{z}_{n'}^{(j)})$, $q_{\text{S}}(\mathbf{y}_{s,n'}^{(j)}, \underline{a}_{ss,n'}^{(j)}, \mathbf{x}_{n'}; \mathbf{z}_{n'}^{(j)}) \triangleq q_{\text{S1}}(\mathbf{y}_{s,n'}^{(j)}, \underline{a}_{ss,n'}^{(j)}, \mathbf{p}_{n'}) q_{\text{S2}}(\mathbf{y}_{s,n'}^{(j)}, \underline{a}_{ss,n'}^{(j)}, \mathbf{x}_{n'}; \mathbf{z}_{n'}^{(j)})$, $q_{\text{D}}(\mathbf{y}_{s,n'}^{(j)}, \mathbf{y}_{s',n'}^{(j)}, \underline{a}_{ss',n'}^{(j)}, \mathbf{x}_{n'}; \mathbf{z}_{n'}^{(j)}) \triangleq q_{\text{D1}}(\mathbf{y}_{s,n'}^{(j)}, \mathbf{y}_{s',n'}^{(j)}, \underline{a}_{ss',n'}^{(j)}, \mathbf{p}_{n'}) q_{\text{D2}}(\mathbf{y}_{s,n'}^{(j)}, \mathbf{y}_{s',n'}^{(j)}, \underline{a}_{ss',n'}^{(j)}, \mathbf{x}_{n'}; \mathbf{z}_{n'}^{(j)})$, and $\bar{q}_{\text{S2}}(\bar{\mathbf{y}}_{m,n'}, \bar{a}_{m,n'}^{(j)}, \mathbf{x}_{n'}; \mathbf{z}_{n'}^{(j)}) \triangleq \bar{q}_{\text{S1}}(\bar{\mathbf{y}}_{m,n'}, \bar{a}_{m,n'}^{(j)}, \mathbf{p}_{n'}) \bar{q}_{\text{S2}}(\bar{\mathbf{y}}_{m,n'}, \bar{a}_{m,n'}^{(j)}, \mathbf{x}_{n'}; \mathbf{z}_{n'}^{(j)})$ respectively, yielding [1, Eq. (17)].

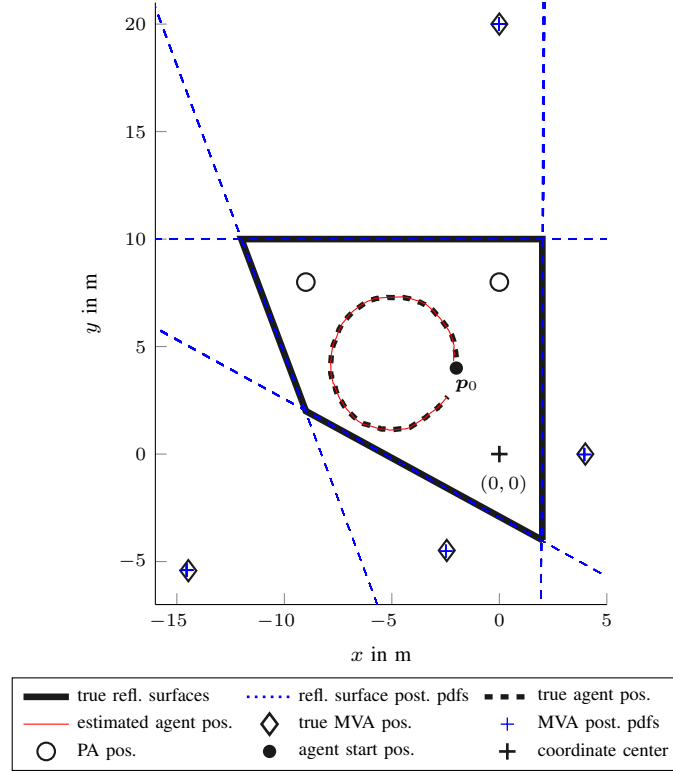


Fig. 1. Considered scenario for performance evaluation in non-rectangular room with two PAs, four reflective surfaces and corresponding MVAs, as well as agent trajectory.

III. ITERATIVE DATA ASSOCIATION

This section contains the detailed messages of Section [1, Sec. V-B6]. Using the messages $\beta(\underline{a}_{ss',n}^{(j)})$ given [1, Sec. V-B4] as well as in [1, Sec. V-B3] and $\xi(\bar{a}_{m,n}^{(j)})$ given in [1, Sec. V-B5], messages $\eta(\underline{a}_{ss',n}^{(j)})$ and $\varsigma(\bar{a}_{m,n}^{(j)})$ are obtained using loopy (iterative) BP. To keep the notation concise, we also define the sets $\mathcal{M}_{0,n}^{(j)} \triangleq \mathcal{M}_n^{(j)} \cup \{0\}$ and $\tilde{\mathcal{D}}_{0,n}^{(j)} \in \tilde{\mathcal{D}}_n^{(j)} \cup \{0\}$. For each measurement, $m \in \mathcal{M}_n^{(j)} \triangleq \{1, \dots, M_n^{(j)}\}$, messages $\nu_{m \rightarrow ss'}^{(p)}(\underline{a}_{ss',n}^{(j)})$ and $\zeta_{ss' \rightarrow m}^{(p)}(\bar{a}_{m,n}^{(j)})$ are calculated iteratively according to [3], [8]

$$\nu_{m \rightarrow ss'}^{(p)}(\underline{a}_{ss',n}^{(j)}) = \sum_{\bar{a}_{m,n}^{(j)} \in \tilde{\mathcal{D}}_{0,n}^{(j)}} \xi(\bar{a}_{m,n}^{(j)}) \psi(\underline{a}_{ss',n}^{(j)}, \bar{a}_{m,n}^{(j)}) \prod_{(s'', s''') \in \tilde{\mathcal{D}}_n^{(j)} \setminus \{ss'\}} \zeta_{s'' s''' \rightarrow m}^{(p-1)}(\bar{a}_{m,n}^{(j)}) \quad (38)$$

$$\zeta_{ss' \rightarrow m}^{(p)}(\bar{a}_{m,n}^{(j)}) = \sum_{\underline{a}_{ss',n}^{(j)} \in \mathcal{M}_{0,n}^{(j)}} \beta(\underline{a}_{ss',n}^{(j)}) \psi(\underline{a}_{ss',n}^{(j)}, \bar{a}_{m,n}^{(j)}) \prod_{m' \in \mathcal{M}_n^{(j)} \setminus \{m\}} \nu_{m' \rightarrow ss'}^{(p)}(\underline{a}_{ss',n}^{(j)}), \quad (39)$$

for $ss' \in \tilde{\mathcal{D}}_n^{(j)}$, $m \in \mathcal{M}_n^{(j)}$, and iteration index $p \in \{1, \dots, P\}$. The recursion defined by (38) and (39) is initialized (for $p=0$) by $\zeta_{ss' \rightarrow m}^{(0)}(\bar{a}_{m,n}^{(j)}) = \sum_{\underline{a}_{ss',n}^{(j)}=0}^{M_n^{(j)}} \beta(\underline{a}_{ss',n}^{(j)}) \psi(\underline{a}_{ss',n}^{(j)}, \bar{a}_{m,n}^{(j)})$. Then, after the last iteration $p=P$, the messages $\eta(\underline{a}_{ss',n}^{(j)})$ and $\varsigma(\bar{a}_{m,n}^{(j)})$ are calculated as

$$\eta(\underline{a}_{ss',n}^{(j)}) = \prod_{m \in \mathcal{M}_n^{(j)}} \nu_{m \rightarrow ss'}^{(P)}(\underline{a}_{ss',n}^{(j)}) \quad (40)$$

$$\varsigma(\bar{a}_{m,n}^{(j)}) = \prod_{ss' \in \tilde{\mathcal{D}}_n^{(j)}} \zeta_{ss' \rightarrow m}^{(P)}(\bar{a}_{m,n}^{(j)}). \quad (41)$$

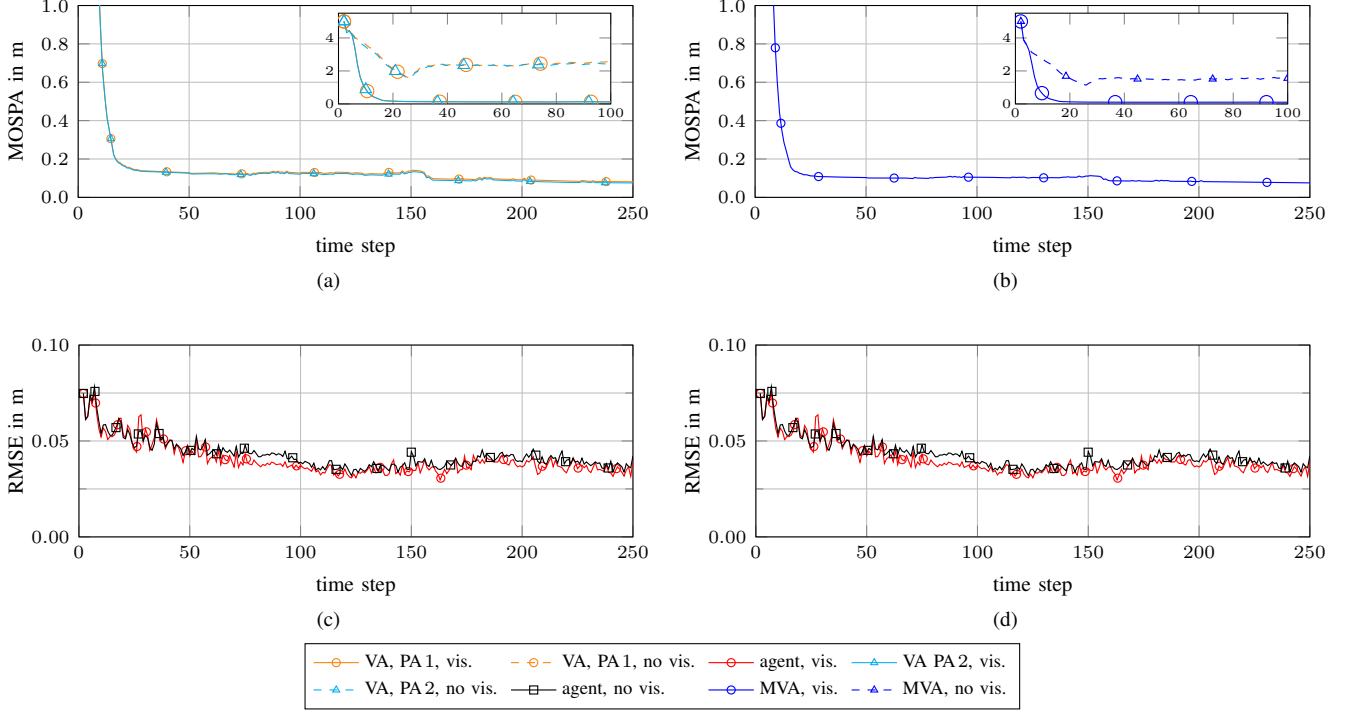


Fig. 2. Performance results: (a) MOSPA errors of the VAs of each PA, (b) MOSPA errors of the MVAs, (c) RMSEs of the mobile agent position, (d) RMSEs of the agent orientation.

IV. ADDITIONAL RESULTS: PERFORMANCE IN NON-RECTANGULAR ROOM

In this section, we provide additional simulation results using synthetic measurements. In particular, this experiment demonstrates the need for an integrated ray-launching to determine the available propagation paths. The setups and parameter are set according to Section [1, Sec. VI-A].

In this experiment, we compare the complete version of the proposed MVA-based SLAM algorithm (vis.), which includes the availability checks as introduced in Sec. [1, Fig. III-D] and Sec. [1, Fig. V-B2], with a reduced variant, where we deactivate availability checks (no vis.), i.e., $p_d(\mathbf{p}_n, \mathbf{p}_{s,\text{mva}}^{(j)}) = p_d(\mathbf{p}_n, \mathbf{p}_{s,\text{mva}}^{(j)}, \mathbf{p}_{s',\text{mva}}^{(j)}) = p_d$. We consider the indoor scenario shown in Figure 1. The scenario consists of four reflective surfaces, i.e., $K = 4$ MVAs, as well as two PAs at positions $\mathbf{p}_{\text{pa}}^{(1)} = [-0.5 \ 6]^T$, and $\mathbf{p}_{\text{pa}}^{(2)} = [4.2 \ 1.3]^T$. The acceleration noise standard deviation is $\sigma_w = 0.02 \text{ m/s}^2$.

Fig. 2a shows the mean optimal subpattern assignment (MOSPA) errors for the two PAs all associated VAs, Fig. 2b shows the MOSPA errors for all MVAs, Fig. 2c shows the root mean-square error (RMSE) of the mobile agent's position, and Fig. 2d shows the RMSE of the mobile agent's orientation, all versus time n . As an example, Fig. 1 also depicts one simulation run of the complete version of the proposed method with availability checks. The posterior PDFs of the MVA positions represented by particles, the corresponding reflective surfaces, and the estimated agent tracks are also shown. The MOSPA errors in Fig. 2a and 2b of the algorithm variant with availability check converge faster and to a much smaller value than those of the variant without availability check. This is because in the scenario investigated, several VAs corresponding to the left as well as the lower walls are not available over large parts of the trajectory (this is the case especially for VAs of $\mathbf{p}_{\text{pa}}^{(2)}$). See also Fig. [1, Fig. 2c], which provides a graphical explanation. Thus, the algorithm variant without availability check tends to deactivate the corresponding MVAs (i.e., strongly lower the probability of existence) as some of the corresponding VAs, which are expected to be detected with p_d are not observed for significant amounts of time. The RMSE of the agent position are not strongly influenced by this deactivation since still sufficient position-related information is provided by the two PAs and the remaining VAs.

REFERENCES

- [1] E. Leitingner, A. Venus, B. Teague, and F. Meyer, “Data fusion for multipath-based SLAM: Combining information from multiple propagation paths,” *ArXiv e-prints*, 2022. [Online]. Available: <https://arxiv.org/abs/2211.09241>
- [2] F. Meyer, P. Braca, P. Willett, and F. Hlawatsch, “A scalable algorithm for tracking an unknown number of targets using multiple sensors,” *IEEE Trans. Signal Process.*, vol. 65, no. 13, pp. 3478–3493, July 2017.
- [3] F. Meyer, T. Kropfreiter, J. L. Williams, R. Lau, F. Hlawatsch, P. Braca, and M. Z. Win, “Message passing algorithms for scalable multitarget tracking,” *Proc. IEEE*, vol. 106, no. 2, pp. 221–259, Feb. 2018.
- [4] E. Leitingner, F. Meyer, F. Hlawatsch, K. Witrissal, F. Tufvesson, and M. Z. Win, “A belief propagation algorithm for multipath-based SLAM,” *IEEE Trans. Wireless Commun.*, vol. 18, no. 12, pp. 5613–5629, Dec. 2019.
- [5] F. Meyer, T. Kropfreiter, J. L. Williams, R. Lau, F. Hlawatsch, P. Braca, and M. Z. Win, “Message passing algorithms for scalable multitarget tracking—supplementary material,” 2018. [Online]. Available: https://winslab.mit.edu/ProcIEEE_MTT_Suppl_Mat.pdf
- [6] Y. Bar-Shalom, X. R. Li, and T. Kirubarajan, *Estimation with Applications to Tracking and Navigation: Algorithms and Software for Information Extraction*. Hoboken, NJ: John Wiley and Sons, July 2001.
- [7] F. Meyer and J. L. Williams, “Scalable detection and tracking of geometric extended objects,” *IEEE Trans. Signal Process.*, vol. 69, pp. 6283–6298, Oct. 2021.
- [8] J. Williams and R. Lau, “Approximate evaluation of marginal association probabilities with belief propagation,” *IEEE Trans. Aerosp. Electron. Syst.*, vol. 50, no. 4, pp. 2942–2959, Oct. 2014.